Soil Properties and Multi-Pollution Affect Taxonomic and Functional Bacterial Diversity in a Range of French Soils Displaying an Anthropisation Gradient

Florian Lemmel, Florence F. Maunoury-Danger, Andrea Fanesi, Corinne Leyval, Aurélie Cebron

Soil properties and multi-pollution affect taxonomic and functional bacterial diversity in a range of French soils displaying an anthropisation gradient

Florian Lemmel[1], Florence Maunoury-Danger[2], Andrea Fanesi[1], Corinne Leyval[1], Aurélie Cébron[1†]

[1] *Université de Lorraine, CNRS, LIEC, F-54000, Nancy, FRANCE*

[2] *Université de Lorraine, CNRS, LIEC, F-57000 Metz, FRANCE*

[†] Corresponding author: aurelie.cebron@univ-lorraine.fr

Abstract

The intensive industrial activities of the 20th century have left behind highly contaminated wasteland soils. It is well known that soil parameters and the presence of pollutants shape microbial communities. But in such industrial waste sites, the soil multi-contamination with organic (polycyclic aromatic hydrocarbons, PAH) and metallic (Zn, Pb, Cd) pollutants and long-term exposure may induce a selection pressure on microbial communities that may modify soil functioning. The aim of our study was to evaluate the impact of long-term multi-contamination and soil characteristics on bacterial taxonomic and functional diversity as related to the carbon cycle.

We worked on 10 soils from northeast of France distributed into 3 groups (low anthropised controls, slag heaps, and settling ponds) based on their physico-chemical properties (texture, C, N) and pollution level. We assessed bacterial taxonomic diversity by 16S rDNA Illumina sequencing, and functional diversity using Biolog® and MicroResp™ microtiter plate tools.

Although taxonomic diversity at the phylum level was not different among the soil groups, many OTUs were influenced by metal or PAH pollution, and by soil texture and total nitrogen content. Functional diversity was not influenced by PAH contamination while metal pollution selected microbial communities with reduced metabolic functional diversity but more tolerant to zinc. Limited microbial utilisation of carbon substrates in metal-polluted soils was mainly due to the nitrogen content. Based on these two observations, we hypothesised that reduced microbial activity and lower carbon-cycle-related functional diversity may have contributed to the accumulation of organic matter in the soils that exhibited the highest levels of metal pollution.

Introduction

The decline of the steel industry in the north east of France at the end of the 20th century left behind more than 6,000 ha of polluted wastelands [1]. On these sites, the soils are multi-contaminated with hydrocarbons and metallic trace elements (MTEs) [2, 3]. On sites of former coking plants or slag heaps, polycyclic aromatic hydrocarbon (PAH) pollution results from the use of coal tar during coke manufacturing. PAHs are ubiquitous contaminants produced from the incomplete combustion of organic matter [4], especially during industrial activities. In settling ponds resulting from the sewage sludge storage of blast furnace gases [5], high concentrations of MTEs (Cd, Cu, Zn, Pb, Ni) are also often encountered.

In soils, the fate of PAHs and MTEs depends on various abiotic and biotic processes. Over time PAHs adsorb onto organic matter and spread into the micropores of soil components. Thus is referred to as the pollutant ageing, and leads to a decrease of pollutant availability [6]. MTE availability depends mostly on soil properties (pH, organic matter, redox potential…) [7, 8]. PAH compounds can be degraded over time mainly through microbial processes [9] that can be limited by low PAH availability [10, 11]. MTEs, cannot be biodegraded, but microorganisms can modify their speciation through direct use or modifications of soil properties [12].

Numerous studies have focused on the short-term influence of PAHs or MTEs on microbial communities. The selective pressure exerted by PAH toxicity [13, 14] could modify microbial community composition [14, 15], reduce microbial taxonomic diversity [16], or inhibit microbial activity and the global activity of enzymes such as arylsulphatase, phosphatase, urease, dehydrogenase [13]. Similarly, various studies have highlighted the negative effects of MTE pollution. For example the effect of zinc addition has been studied on enzymatic activity and microbial community composition [17], as well as on the taxonomic diversity of bacterial communities [18].

In aged polluted soils, various adaptation processes enable the microbial community to cope with and even benefit from pollution. The selection of PAH degraders [15, 19] and MTE-resistant microbes [17, 20] in aged-polluted soils has been shown using acquired tolerance tests [21]. However, the long-term impact of chronic exposure to PAHs and MTEs on microbial community composition has been less addressed [22, 23]. The impact of pollutants has been mainly studied separately, although multi-contamination can have a synergistic effect [24, 25]. Studies considering aged pollution and the impact of multi-contamination on microbial taxonomic diversity (richness and evenness) are scarce [26] and therefore needed.

The carbon cycle is pivotal in soil functioning because it contributes to all biological processes, such as biomass production or respiration by organisms. It also affects other nutrient cycles through organic matter recycling and mineralisation. In a context of soil pollution, one can thus wonder how the different functions of the carbon cycle are affected, and study the microbial functions involved in key C-cycle processes. Metabolic functional diversity can be defined as the number (richness) and the evenness of the metabolic functions of the microbial community. One approach to estimating functional diversity is by comparing the degradation capacities of carbon substrates using Biolog® [27] and MicroResp™ [28] microtiter plate methods in the presence or absence of pollutants, as done with metals that decrease bacterial functional diversity [29].

Apart from this impact of pollutants, it is well known that soil parameters, such as the pH, texture, the C content or the C/N ratio, highly contribute to shape microbial community composition [30, 31] and functional

diversity [32] in soils of various origins (forest, grassland, agricultural…). In polluted soils, such as urban, industrial, traffic, mining and military areas [3], physico-chemical parameters have also been found to largely influence the composition of the bacterial and fungal communities [22].

We therefore hypothesised that microbial diversity in multi-contaminated soils may be influenced by both soil properties and pollutant concentrations and availability, but differently at the taxonomic and functional levels. In this context, the present study aimed to: i) assess taxonomic diversity and metabolic functional diversity of microbial communities in a context of aged multi-pollution, and ii) to determine which soil factors (physico-chemical parameters, pollutants…) affected these diversities. We studied microbial communities from a collection of 10 soils presenting gradients of PAH and metal pollution, and under different land uses, ranging from weakly to highly anthropised, i.e. from forest soil to industrial soil. We assessed bacterial taxonomic diversity through 16S rRNA gene tag-amplicon sequencing (Illumina MiSeq). We estimated metabolic functional diversity using the degradation functions of ecologically relevant carbon substrates through Biolog® and MicroResp™ microtiter plate methods.

Materials and methods

Study sites and soil sampling

Ten soils originating from industrial wastelands and waste sites, natural forests or ancient gravel pit, located in the "Grand Est" region (north-east of France), were sampled in November 2015. This soil collection was chosen to cover a wide range of anthropisation situations, i.e. from no or low contamination to high contamination, and represented an anthropisation gradient. All sampling sites are within 100km. Three soils were considered as the control soils (*ctrl*), i.e. two low-anthropised forest soils collected at Hémilly (*He*; 49°2'1"N/6°30'51"E; Moselle; Stagnic Luvisol) and Montiers-sur-Saulx (*Mo*; 48°31'55"N/5°16'8"E; Meuse; Calcaric Cambisol), and one anthropised but unpolluted former gravel pit soil collected at Dieulouard (*Di*; 48°49'44"N/6°5'2"E, Meurthe-et-Moselle; Fluvisol). Seven anthropised soils (Technosol) known to be polluted by MTEs and/or PAHs, where industrial activities stopped during 1980s, were collected from: i) former slag heaps (*sh*) at Homécourt (*Ho*; 49°12'79"N/5°59'72"E, Meurthe-et-Moselle), Terville (*Te*; 49°20'25"N/6°08'33"E; Moselle), Uckange (*Uc*; 49°18'58"N/6°9'55"E; Moselle), and Neuves-Maisons (*NM*; 49°12'52"N/5°59'45"E; Meurthe-et-Moselle), and ii) former settling ponds (*sp*), dried since at least 30 years, at Pompey (*Po*; 48°46'8"N/6°8'8"E; Meurthe-et-Moselle), Mont-St-Martin (*MsM*; 49°32'9"N/5°46'46"E; Meurthe-et-Moselle), and Russange-Micheville (*RM*; 49°28'58"N/5°55'51"E; Moselle).

All sites were colonized by trees (mainly birch and/or beech) and herbaceous plants, with a very heterogeneous colonization density from one site to another, except for the NM soil which was colonized only by some herbs. None of the soil samples were rhizosphere soils or directly under plant influence (sampling at least 2m from a tree). As plant colonization was sparse by location, we collected samples on bare soils. At each of the ten sites, samples were collected from three independent sub-sites 1 m apart. After removing the litter layer, if present, one soil block per sub-site (block of 20 cm on the side and 30 cm deep) was removed using shovel. The three sub-site soil blocks were mixed to get one composite sample *per* site. Back to the laboratory, the soil samples were air-dried at room temperature for one week, and then sieved at 2 mm. The dried and sieved soils were then stored at room temperature in the dark before chemical and microbiological analyses, and aliquots were stored at -80 °C before freeze-drying and PAH analyses.

Soil physico-chemical characteristics

The soil physico-chemical characteristics were determined from the dried sieved soils. The pH was measured (PHM210 Radiometer Analytical, equipped with a pH probe, Bioblock Scientific) in a soil suspension prepared in distilled water (1:5 w:v). The $CaCO_3$ content was estimated from measurements of CO_2 concentrations released after acid (4M HCl) decarbonation of 1 g of dw soil, using an infrared absorbance (Binos 1004 analyser), with λ 2325.6 cm^{-1}. The water retention capacity was estimated from the difference in weight between dry and water-saturated soil, which corresponded to 100%. Measurements of the soil texture (clay fraction, 0-2 µm; silt fraction, 2-63 µm; sand fraction 63-2,000 µm; ISO 11277), the cation exchange capacity (CEC; determined by Metson method, NF X 31-130), organic carbon, organic matter, nitrogen concentrations (C, OM, and N,

respectively; Dumas method, ISO 10694), the available phosphorus concentration (P; Olsen method, NF ISO 11263), total (fluoridric acid extraction) and available (calcium chloride extraction) concentrations of metals (Cr, Cd, Cu, Ni, Pb, Zn for total and available concentrations, plus Tl, Mo, Al, Ca, Fe, K, Mg, Mn, and Na for total concentrations) were performed at the laboratoire d'analyse des sols (INRA, Arras, France).

We calculated a metal pollution index (Mi) in order to compare metallic pollution of soils using only one variable. Mi was the sum of the relative proportions (RP_{metal}) of nine metal concentrations (Zn, Pb, Cd, Fe, Cr, Cu, Ni, Co, Tl). RP_{metal} in soils were calculated using the following formula:

$$RP_{metal} = \frac{MC_{soil} \times 100}{MC_{max}}$$

where MC_{soil} is the total metal concentration in the soil, and MC_{max} is the maximum total metal concentration found among all the soils of the collection. Total instead of available metal concentrations were used because some of the available metal values were lower than the detection limit. The nine metals were chosen because they commonly resulted from the steel industry, and when for at least one soil, the metal concentration was higher than the mud compost norm (NF 44 095) or the natural geochemical background of French soils [33].

PAH extraction and analysis

Soil samples stored at -80 °C were freeze-dried and ground to 500 µm (Mixed Mill MM 400, Retsch). Total PAHs were extracted from 1 g dw soil in triplicate with dichloromethane, at 130 °C and 100 bars, using accelerated solvent extraction (DIONEX® 200 ASE), as described in Cennerazzo et al. [34]. Available PAHs were extracted from 1 g dw soil in triplicate with 20 ml of hydroxypropyl-β-cyclodextrin (50 mM) in Teflon™ FEP Oak Ridge centrifuge tubes (Nalgene, USA) [35]. After mixing (16 h) at 24 °C and centrifugation, PAHs were extracted from the aqueous solution through liquid:liquid extraction using dichloromethane. Both solvent extracts of total and available PAHs were evaporated (nitrogen flow) and dissolved in acetonitrile for PAH analysis using a reverse-phase chromatography (UHPLC DIONEX® Ultimate 3000 system) equipped with a Diode Array Detector (UV detection, 254 nm) and a Zorbax Eclipse PAH column (2.1 x 100 mm, 1.8 µm, Agilent).

Carbohydrate, organic acid, and dissolved organic carbon measurements

Carbohydrates, organic acids, and dissolved organic carbon (DOC) were measured on triplicate soil aqueous extracts (1:5 w:v) using 6 g dw soil mixed with 30 ml of distilled water in Teflon™ FEP Oak Ridge centrifuge tubes (Nalgene, USA) for 2h at 20 °C [36, 37]. After centrifugation and filtration, aqueous extracts were recovered. Seven carbohydrates (inositol, trehalose, sucrose, glucose, xylose, mannose, and fructose) were quantified by an ICS 3000 ion-exchange chromatograph equipped with a Dionex CarboPac SA10 column (Thermo Scientific). Eleven organic acids (gluconic, lactic, acetic, propionic, formic, pyruvic, succinic, maleic, oxalic, fumaric, and citric acids) were quantified using an ICS 2100 ion chromatographer equipped with a Dionex IonPac AS11 HC column (Thermo Scientific). DOC was measured on a TOC-V analyser (Shimadzu).

Quantification of culturable bacteria

The most probable number (MPN) was measured on 1 g dw soil (in triplicate) moistened (to 60% of their water retention capacity) and pre-incubated for 2 days (24°C) for reactivation of microbial community. After soil aliquots were resuspended in 10 ml of NaCl (0.9%) and mixed for 1 h, ten-fold dilution series were prepared in NaCl (0.9%) and used to inoculate 96-well microtiter plates (16 wells *per* dilution) filled with nutrient Broth No 1 (Fluka analytical). After incubation for 3 days (24 °C), absorbance at 600 nm was measured using spectrophotometer (Safas, Monaco) and MPN counts were calculated using Mac Grady's tables, and expressed as MPN *per* gram of soil.

DNA extraction, real-time quantitative PCR, and sequencing

Genomic DNA (gDNA) was extracted in triplicate from *ca.* 0.5 g of moistened soil (as described above) stored at -20 °C, using Fast DNA Spin Kit for Soil (MP Biomedicals, France), following the manufacturer's instructions. Concentration and purity (A_{260}/A_{280} ratio) were measured using a spectrophotometer (UV1800, Shimadzu) equipped with a TrayCell™ adapter (Hellma®). gDNA was diluted to 5 ng μl^{-1} for real-time quantitative PCR (qPCR) and sequencing library preparation. The abundance of fungi and bacteria was estimated by qPCR using the primer sets Fung5F/FF390R [38], 968F/1401R [39], targeting 18S and 16S rRNA genes, respectively. The qPCR assays were performed as previously described [40, 41]. Briefly, the reaction mixture (20 µl) was composed of 10 µl iQ SYBR green SuperMix (Bio-Rad), 0.8 µl primers (10 µM), 0.4 µl bovine serum albumin solution (3%), 0.2 µl dimethyl sulfoxide, 0.08 µl T4gp32 (MP Biomedicals, France), and 1 µl DNA (diluted gDNA or 10-fold dilution series from 10^8 to 10^1 copies μl^{-1} of the standard plasmids). Quantification was performed using a CFX96 Real-Time PCR detection system (Bio-Rad), using 56 °C and 50 °C as annealing temperature for 16S and 18S rDNA quantification, respectively.

The V3/V4 region of bacterial 16S rRNA genes (*ca.* 550 bp) was amplified using primers S-D-Bact-0341-a-S-17 and S-D-Bact-0787-b-A-20 [42, 43] and following a previously described dual-index strategy [44] using PCR primers with Illumina adaptor, pad and index sequences [37]. PCR reactions were performed on 2 µl of diluted gDNA using Phusion high-fidelity polymerase (Thermo Scientific). PCR reactions consisted of 31 cycles with touchdown annealing temperature for 18 cycles (63 °C to 54°C with a decrease of 0.5 °C/cycle) and 13 cycles at 54 °C. Amplification products were checked on 1% agarose gel electrophoresis, and purified using the UltraClean-htp 96 Well PCR Clean-Up kit (Qiagen) following the manufacturer's instructions. After Quant-iT Picogreen ds-DNA assay Kit (Invitrogen) quantification, an amplicon library was prepared (equimolar pool at 10 nM), purified on a QIAquick PCR purification kit column (Qiagen), and sent for sequencing to Genewiz platform (South Plainfield, NJ, USA) using an Illumina MiSeq V2 Kit for 2 x 250 bp paired-end sequencing. Illumina MiSeq paired-end reads have been deposited in the SRA database under Bioproject accession number PRJNA450766. Sequence data were analysed following the MiSeq SOP procedure available in March 2017 and described in Kozich et al. [44], using Mothur v.1.38.0 [45]. Paired-end reads were trimmed using the following criteria: QS>20, 404 bp < length < 454 bp, and no ambiguous bases. Chimeras detected using Uchime [46] and singletons (sequences appearing only once among all samples) were removed. Alignment of unique sequences and taxonomy was assigned using the Silva bacteria database (cutoff = 80).

Sequences affiliated to archaea, eukaryota, unknown, mitochondria, and chloroplasts were removed. Sequences were clustered in Operational Taxonomic Units (OTUs) at 97% similarity. Finally, datasets were rarefied to the lowest number of sequences *per* sample (34 191 reads/sample). Alpha diversity was expressed by calculating Chao1, Pielou's evenness J', and Shannon H' indices [47] and Beta-diversity was calculated with Bray-Curtis index, using Mothur.

Carbon substrate utilisation using Biolog® plates and metal tolerance test

Two types of Biolog® microtiter plates were used to assess the metabolic functional diversity of bacterial communities through utilisation patterns of 62 carbon substrates (Table S1): i) EcoPlates™ containing 31 substrates of ecological relevance (5 guilds: 9 carboxylic acids, 6 amino acids, 8 carbohydrates, 4 polymers, and 4 miscellaneous), and ii) MT2 microplates™ allowing to test 31 chosen substrates (4 PAHs, 6 aromatic acids, 8 carboxylic acids, 3 amino acids, 6 carbohydrates, 3 polymers, and 1 miscellaneous). MT2 microplates™ were prepared following the manufacturer's instructions (0.3 mg of carbon in each well) except for organic acids, cellulose, and lignin which were 10-fold diluted because the recommended concentrations were toxic or the presence of solid particles flawed absorbance measurements (data not shown). PAHs and phenolic acids were dissolved in n-hexane and added to empty plates, and the solvent was eliminated by drying for 12 h in a sterile hood [37]. The water-soluble substrates (20 µl) were added just before inoculation and 20 µl of sterile water were added in the wells containing PAHs and phenolic acids and in the EcoPlate™ wells.

Microbial inocula were prepared by diluting soil aliquots (1 g of moistened soil prepared as described above) in 10 ml of NaCl (0.9%) and stirring with glass beads (1.5-mm diameter) for 1 h. Supernatant was decanted for 15 min and diluted in NaCl (0.9%) differently for each soil, based on MPN data to obtain a similar microbial abundance (from 10^2 to 10^3 cultivable bacteria ml^{-1}) for all soil. Biolog® plates were inoculated with 100 µl of the appropriate dilution, and incubated at 24 °C in a plastic bag containing wet cotton to avoid desiccation.

Zinc was used to test bacterial community tolerance to metals. Biolog® substrate utilisation was measured in the presence of zinc, added as $ZnCl_2$ (10 mg l^{-1} of Zn) directly in the inoculum. This zinc concentration was chosen to obtain a zinc effect without total inhibition of bacteria (preliminary experiments not shown).

To summarise, our experimental design tested 62 carbon substrates on 10 soils in triplicate, with or without zinc addition. The absorbance at 595 nm was monitored in an spectrophotometer (SAFAS, Monaco) over 7 days at t = 0, 24, 48, 72, and 96 h. Absorbance values were corrected (Abs_{corr}) after subtraction of the absorbance of mean blank wells at the corresponding times. Substrate utilisation was considered positive when the corrected absorbance was > 0.2. For each soil, Abs_{corr} at 96 h was used to calculate functional alpha diversity estimators, i.e. metabolic richness (number of carbon substrates significantly utilised), Pielou's evenness (J'; based on the relative proportions of utilisation intensity for each substrate) and Shannon (H'; based on the two previous indices) diversity indices using the vegan package in R [48]. For each soil, the average well color development (AWCD) was calculated over time using the formula:

$$AWCD = \frac{\sum bs_{corr}}{62}$$

where Abs_{corr} was the corrected absorbance of the substrate. Zinc tolerance was assessed for each soil by calculating a percentage of inhibition based on a comparison of areas below the AWCD curves between conditions with or without zinc. Percentages of inhibition were compared to soil total and available zinc concentrations (transformed to 1 when below the detection limit, i.e. 10 µg kg^{-1}) through linear regressions.

Soil metabolic profiling using the MicroResp™ method

The MicroResp™ technique was used to measure basal respiration and substrate-induced respiration (SIR) [28]. Soils were loaded (four replicates) into the 96-deep-well plates, and the mean mass of each soil was measured. Soils were moistened to 45% water retention capacity using sterile distilled water, and plates were pre-incubated 3 days at 24 °C in a plastic bag containing wet cotton to avoid desiccation. After this step, six carbon sources (pyruvate, succinate, citrate, L-asparagine, D-ribose, and D-mannitol), selected according to the contrasting levels of substrate utilisation in Biolog® plates among soils, were added to reach 80% of soil water retention capacities. Substrates were added at 20 mg of C per well except for L-asparagine (3 mg) and citrate (5 mg) having lower solubility. Water was added to plates for basal respiration. Finally, deep-well plates were sealed to the CO_2-trap microtiter plates and incubated in the dark at 24 °C for 4 to 9 h depending on the carbon source (Table S1) and for 8 h for basal respiration. Absorbance was measured at 570 nm using an spectrophotometer (SAFAS, Monaco) just before sealing to measure blank values to subtract to the final absorbance. Mean basal respiration (n = 8) was measured on two independent series and 6 SIR were measured on 4 replicates for the 10 soils. Absorbance values for SIR were corrected by subtracting the absorbance mean (n = 4) of the corresponding soil basal respiration series, and transformed into a CO_2 concentration using the following formula:

$$ppm\ of\ C02\ = 138.72 \times \exp^{(6.7974 \times ODC)}$$

where *ODc* is the corrected absorbance. Then the CO_2 concentration was standardised by dividing it by the soil quantity and the incubation time. Based on MicroResp instruction manual, ppm values of CO_2 were then expressed as quantity of carbon released as CO_2 per gram of soil per hour. For each soil, these corrected and standardised absorbance values were used to calculate the same functional diversity estimators (richness, evenness, and Shannon diversity indices) as the ones described above for Biolog data.

Statistical analyses

All statistical analyses were performed using RStudio v1.0.136. Significant differences among soils or among soil groups were assessed using Kruskal-Wallis rank sum test followed by a multiple comparison test included in the Vegan R package [48]. For principal component analysis (PCA) nine soil variables among soil physico-chemical, pollution, and texture characteristics, were used, and soil groups were made with Monte Carlo test using 1,000 iterations. For redundancy analysis (RDA), explanatory variables were chosen by using the *ordistep* R function. Permutation tests on the RDA axes and variables were performed. Multivariate analyses were carried out on

standardised data using the ade4 [49] and vegan R packages. Linear regression was assessed by fitting to a linear model using "lm" function. The partial least square regression (PLSr) algorithm [50, 51] in regression mode was used to identify possible relationships between the soil physico-chemical characteristics and 96 bacterial OTUs (each representing at least 1% of the total). The two matrices were z-normalised. The PLSr was implemented using the mixOmics package [52, 53]. Once calibrated, the PLSr model was validated using the leave-one-out cross-validation method. The R^2 and the mean squared error of prediction were then used (data not shown) to select the appropriate number of principal components used to implement the model. The correlation between bacterial OTUs and soil physico-chemical parameters was displayed in a heatmap ("cim" function) resulting from the similarity matrix obtained from the PLSr model.

Results

Grouping of soils according to their physico-chemical characteristics

The physico-chemical and microbial characteristics of the ten soils are summarised in Table 1 and 2. Many characteristics differed among soils and soil groups (settling pond, slag heap, control). Although one of the control forest soils (ctrl-He) had a pH of 5.4 while all other soils had a slightly basic pH (from 7.0 to 8.0), no statistical pH difference was observed among the soil groups. The slag heap soils differed by a high available PAH concentration and intermediate values of the metal pollution index, whereas the settling pond soils had a high metal pollution index with especially high Zn, Pb, Cd, and Tl concentrations and intermediate values of available PAH concentrations. These two groups also presented high total PAH concentrations and high Fe concentrations as compared to the control soils. The control soils were mainly characterised by the highest dissolved organic carbon concentration and the lowest total PAH concentration and metal pollution index. The control soils also contained higher total potassium and aluminium concentrations than the other soils, probably in part due to their proportion of clay. No difference among soil groups was observed for the C/N ratio or for concentrations of total organic carbon, organic matter, nitrogen, organic acids, carbohydrates, and available phosphorus. Our collection of soils also presented highly variable iron concentrations, ranging from 18 g kg^{-1} in ctrl-Di to a particularly high concentration of 452 g kg^{-1} in sh-Uc. Concerning microbial parameters such as MPN counts and 16S rRNA gene abundance, soil groups were not statistically different. Interestingly, the ratios of fungal to bacterial abundance (18S /16S rDNA ratios) were similar between the control and slag heap soils, and the lowest for settling pond soils, probably because the three soil groups had similar 18S rRNA gene copy numbers while the settling pond soils tended to have higher 16S rRNA gene copy numbers ($p = 0.053$).

We performed a PCA on the basis of soil physico-chemical, pollution, and texture characteristics (Fig. 1), which confirmed the distribution of the 10 soils in 3 groups based on their use. The first three components of the PCA explained 76.75% of total variance, with the first (PC1), the second (PC2) and the third (PC3) components of the PCA accounting for 35.3%, 28.5%, and 12.8%, respectively. The main contributing variables were the metal pollution index Mi (24.8% of total variance on the considered axis) and the total potassium concentration (18.9%) on the first axis, soil texture (sand: 33.1%; clay: 24.9%) and the pH (13.8%) on the second axis, and PAH (46.9%) and organic carbon (30.9%) concentrations on the third axis (not shown). On PC1, control soils were mainly separated from slag heap and settling pond soils by the potassium and clay fraction parameters. Interestingly, settling pond soils were separated from the control and slag heap soils by the metal pollution, organic carbon, and nitrogen parameters. On PC2, slag heap soils were separated from the control and settling pond soils by the sand fraction and pH parameters. PAH pollution was not a discriminative parameter (10.6% of the weight on PC2) and did not separate the soil groups according to their use on the PC3 axis (46.86% of the weight on PC3). To test if the soil groups were robust, we performed a Monte-Carlo test, and confirmed that our grouping was statistically significant (1,000 iterations, $p = 1.998 \times 10^{-3}$). We also performed a second PCA without the pollution characteristics (data not shown) and confirmed the separation of the soils in three groups corresponding to their use (Monte Carlo test, 1000 iterations, $p = 0.016$).

Bacterial taxonomic diversity

We determined bacterial taxonomic diversity by sequencing 16S rRNA genes. After read treatment and rarefaction to 34,191 reads *per* sample, we classified OTUs with 97% similarity taxonomically. The taxonomic alpha diversity estimators based on OTU data are shown in Table 2. Interestingly, slag heap soils harboured more diversified bacterial communities with higher Shannon's diversity (mean value of 6.203) and Pielou's evenness (mean value of 0.791) indices than settling pond soils. Compared to the other two soil groups, control soils had similar bacterial taxonomic diversity indices due to the low and high bacterial taxonomic diversity indices of ctrl-Mo and ctrl-Di, respectively. We investigated bacterial taxonomic diversity at the phylum level (Alpha, Beta, Gamma, and Delta classes were found for Proteobacteria). Their relative proportions in each soils are presented in Fig. 2. Based on the dissimilarity distance matrix, the soils were all highly different: the minimum Bray-Curtis dissimilarity index between two different soils was 0.814, while it ranged from only 0.254 to 0.519 for replicates of a same soil (data not shown). Phylum proportions varied among soils, with a majority of Acidobacteria, Actinobacteria, and Proteobacteria. Acidobacteria were dominant (10.8% to 31.4%), except in ctrl-Mo (7.1%) and sh-NM (4.3%) communities. Within the soil collection, Actinobacteria represented 10.1% to 25.9% of bacterial communities. Proteobacteria represented 16.2% to 35.1% of soil bacterial communities and were mainly represented by Alpha-Proteobacteria (up to 18.5% in sh-Te), except in ctrl-Mo where Beta-Proteobacteria were the dominant proteobacterial class and represented 13.2%. We can note that ctrl-He, sp-MsM, and sp-RM bacterial soil communities harboured the lowest proportions of Proteobacteria but high proportions of Verrucomicrobia (22.1% in ctrl-He) and of unclassified OTUs (16.5% and 17.8% in sp-MsM and sp-RM, respectively). Bacterial communities from soils sharing the same use had very different compositions. For example, Firmicutes represented 13.8% of the sp-MsM soil community, while they represented a maximum of 0.4% of the other settling pond soil bacterial communities. By comparing soil groups, we noted that Verrucomicrobia were present in a significantly higher proportion in control soils than in polluted soils ($p = 9.415 \times 10^{-5}$). On the contrary, polluted soils harboured a significantly higher proportion of Candidate division TM7 phyla than control soils ($p = 0.001$). We investigated the relationship between physico-chemical soil parameters and bacterial phylum proportions by searching significant linear correlations. The proportion of Actinobacteria was positively correlated to the total nitrogen concentration (Pearson, $p = 6.74 \times 10^{-4}$, $r = 0.88$) and the soil cation-exchange capacity (Pearson, $p = 2.04 \times 10^{-3}$, $r = 0.85$). The proportion of Proteobacteria was positively correlated to total and available PAH concentrations (Pearson, $p = 1.59 \times 10^{-3}$, $r = 0.86$, and $p = 9.99 \times 10^{-4}$, $r = 0.87$, respectively), mostly due to a correlation with gamma-Proteobacteria (Pearson, $p = 0.05$, $r = 0.63$, and $p = 0.02$, $r = 0.71$, respectively). Positive correlations between the proportion of Chloroflexi and total zinc and lead concentrations (Pearson, $p = 2.43 \times 10^{-3}$, $r = 0.84$, and $p = 0.03$, $r = 0.70$, respectively) were also found. The proportion of unclassified OTUs was correlated with the total zinc concentration (Pearson, $p = 5.42 \times 10^{-3}$, $r = 0.80$) and the metal pollution index (Pearson, $p = 1.93 \times 10^{-2}$, $r = 0.72$). Similarly, the proportion of Gemmatimonadetes was positively correlated with the metal pollution index (Pearson, p =

344 1.44 x 10^{-2}, r = 0.74) and with various metals such as total nickel and cobalt concentrations (Pearson, p = 1.66 x
345 10^{-2}, r = 0.73, and p = 1.52 x 10^{-2}, r = 0.74, respectively).
346 The analysis at the OTU level generated 32,920 OTUs, which ranged from 2,159 (sp-RM) to 4,434 (ctrl-Di) mean
347 OTUs *per* sample. The PLSr was computed to gain insights into the soil physico-chemical parameters that drove
348 bacterial taxonomic diversity. The heatmap in Fig. S1 shows that the distribution of correlations between
349 bacterial diversity and soil characteristics was rather scattered, reflecting a great heterogeneity of the
350 relationships linking bacterial diversity to soil properties. Each soil factor selectively correlated only to a small
351 number of OTUs (10-17). In particular, as identified by the high correlation coefficients (> 0.9), the strongest
352 correlations between soil properties and OTUs concerned the pH, the clay content, and the PAH content.
353 Whereas the pH and clay seemed to correlate mostly to OTUs affiliated to the Verrucomicrobia (negatively) and
354 Firmicutes (positively), respectively, the PAH content appeared to affect a more diverse range of OTUs. The soil
355 PAH content was indeed positively and strongly correlated to the abundance of 5 OTUs affiliated to
356 Bacteroidetes (*Flexibacter* and *Flavobacterium* members) but also to that of 3 OTUs affiliated to Chloroflexi,
357 and 4 affiliated to Alpha-Proteobacteria (2 OTUs belonging to *Sphingomonadaceae*), Nitrospirae, and
358 Actinobacteria (one OTU affiliated to *Arthrobacter*). Interestingly, these groups were mostly unaffected by all
359 other soil parameters and were the only taxa affected by PAHs. Moreover, no OTU was negatively affected by
360 PAHs. With respect to the other soil characteristics such as total N, available P, and the metal concentration
361 index, we observed weaker correlations with bacterial diversity. These factors were positively correlated to one
362 group of OTUs dominated by members of Actinobacteria. The total organic carbon and sand contents were
363 slightly correlated to 2 other groups of OTUs, but with opposite effects. Organic C was positively correlated to a
364 highly diversified taxonomic group, while the sand content was positively correlated with a group of 8
365 Acidobacteria.
366

367 **Metabolic functional diversity**

368 The soil basal respiration and the substrate-induced respiration (SIR) measured for six different carbon sources
369 (L-asparagine, citrate, succinate, pyruvate, D-mannitol, D-ribose) using MicroResp microtiter plates are shown
370 in Fig. 3. The functional alpha diversity estimators based on MicroResp data are shown in Table 2. No statistical
371 difference among soil groups emerged for substrate richness, probably due to the low number of carbon
372 substrates we tested. The control and slag heap soils had similar functional Shannon indices and higher ones
373 than the settling pond soils. Pielou's functional evenness index was statistically different among the 3 soil
374 groups, with the highest for slag heap soils and the lowest for settling pond soils. The sum of SIRs for the 6
375 different carbon sources was used as a proxy of the soil metabolic activity (Fig. 3). Most of the carbon sources
376 were utilised by every soil, i.e. the SIR level was higher than basal respiration, except with D-mannitol that was
377 not utilised by sh-Te, and citrate that was not utilised by ctrl-Mo, ctrl-Di, sh-Ho, and sp-Mi. The highest
378 measured SIR was with pyruvate and the lowest with citrate. sp-Po showed the highest metabolic activity,
379 while sh-Ho showed the lowest, mostly due to the great differences in SIR levels with the pyruvate substrate
380 (data not shown). Kruskal-Wallis tests showed that all SIR values except with D-ribose significantly differed

among the soils. Based on soil groups, Kruskal-Wallis tests revealed that the settling pond soils had a significantly higher soil metabolic activity than the slag heap and control soils ($p = 1.93 \times 10^{-3}$), mostly due to the high metabolic activity of sp-Po. Basal respiration and SIR with pyruvate were also the highest in the settling pond soils and the lowest in the slag heap soils ($p = 1.73 \times 10^{-7}$ and $p = 9.54 \times 10^{-5}$, respectively). Finally, a positive linear correlation (Pearson, $p = 6.99 \times 10^{-5}$, $r = 0.94$) was found between soil metabolic activity and soil basal respiration. Additionally, these last two parameters were positively correlated with the total nitrogen concentration (Pearson, $p = 8.42 \times 10^{-3}$; $r = 0.77$, and $p = 1.53 \times 10^{-2}$; $r = 0.74$, respectively).

We assessed carbon substrate utilisation using Biolog microtiter plates to calculate soil metabolic richness and average well colour development (AWCD) (Fig. 4). The functional alpha diversity estimators based on Biolog data are shown in Table 2. Kruskal-Wallis test showed that bacterial communities from the settling pond soils had a significantly lower metabolic richness and Shannon's diversity indices than bacterial communities from the slag heap and control soils, while no difference among the three soil groups was observed for Pielou's evenness index. The metabolic richness of the ten soils ranged from 5 (sp-RM) to 31 (ctrl-Mo) utilised carbon sources, out of a total of 62 carbon sources. None of the 10 soils significantly catabolised PAHs in the conditions of the experiment, probably due to a too short incubation time. Thus, except PAHs for all soils, and polymers and miscellaneous substrates for sp-RM, at least one substrate from each substrate guild was utilised by each soil. Among the 62 carbon substrates, protocatechuic acid, L-asparagine, Tween 40, D-mannitol, succinic acid, and putrescine were the best utilised carbon substrates in the aromatic acid, amino acid, polymer, carbohydrate, carboxylic acid, and miscellaneous guilds, respectively. On the contrary, for these same carbon guilds, the less utilised substrates were syringic acid, glycine, alpha-cyclodextrin, D-sucrose, propionic acid, and pyrocatechol, respectively. Kruskal-Wallis tests showed significant differences in metabolic richness among soils, especially between ctrl-Mo and sp-RM. ctrl-Mo indeed exhibited higher total metabolic richness and a wider range of utilised carboxylic acids, carbohydrates, and polymers than sp-RM. No significant difference was observed among soils for miscellaneous, amino acid, and aromatic acid metabolic richness. Besides, as regards the soil groups, the settling pond soils showed significantly lower total metabolic richness ($p = 0.007$), carboxylic acid ($p = 0.017$) and carbohydrate ($p = 0.004$) utilisation richness than the slag heap and control soils. Regarding utilisation of substrates from the polymer guild, the settling pond soils showed the lowest metabolic richness, and the control soils the highest ($p = 0.03$), respectively. Finally, a positive linear correlation (Pearson correlation, $p = 1.182 \times 10^{-5}$, $r = 0.959$) was found between total metabolic richness and AWCD.

Zinc tolerance

Soil microbial zinc tolerance was assessed using Biolog microtiter plates by adding $ZnCl_2$ solution, and then percentages of inhibition due to zinc addition were calculated. Fig. 5 shows the linear regression between the soil available zinc concentration and the percentage of inhibition of carbon substrate utilisation. A similar linear regression was found with the total zinc concentration ($p = 3.975 \times 10^{-5}$, $R^2 = 0.45$). The settling pond soils had the highest available zinc concentration, and their metabolic activity was the least inhibited by zinc addition.

418 The ctrl-He soil also had a high available zinc concentration (38.1 mg kg^{-1}), due to its low pH (5.4, Table 1)
419 leading to a higher MTE availability and a lower zinc inhibition of metabolic activity (46.2%). In comparison, ctrl-
420 Mo and ctrl-Di had neutral pH values (7.0 and 7.3, respectively), a low available zinc concentration (< 10 and 11
421 µg kg^{-1}, respectively) and a higher zinc inhibition of metabolic activity (49.3 and 54.7%, respectively).
422
423 **Effects of the soil characteristics on taxonomic and metabolic functional diversity**

424 We investigated the effects of soil environmental characteristics on bacterial taxonomic diversity (Fig. 6A), and
425 MicroResp (Fig. 6B) and Biolog (Fig. 6C) metabolic functional diversity through redundancy analyses. We
426 performed three RDAs using soil environmental characteristics as explanatory variables, and the taxonomic and
427 functional diversity indices of the soil microbial communities (Table 1 and 2) as response variables. The
428 explanatory variables that best explained the variation of diversity indices were selected by backward selection
429 to maximise the percentage of explained variability leading to at least 99.3% of total variation. The
430 supplemental Table S2 provides p values and coefficients for axes and soil properties significance. Only the first
431 axis ($p < 0.005$) in Fig. 6A and 6B was significant, and so were the first two axes ($p < 0.005$ and $p < 0.02$) in Fig.
432 6C. Among the explanatory variables (metal pollution index, PAH concentration, pH, and sand fraction), only
433 the sand fraction had a significant effect (first axis; Fig. 6A) on bacterial taxonomic diversity ($p < 0.01$, $F = 16.30$). This relationship was confirmed by significant positive linear correlations between the proportions of
435 soil sand fractions and Chao1 ($p = 5.97 \times 10^{-3}$, $r = 0.80$), Shannon diversity ($p = 3.50 \times 10^{-3}$, $r = 0.82$) and Pielou's
436 evenness ($p = 0.01$, $r = 0.76$) indices. Total organic carbon and nitrogen concentrations were the two
437 significantly explanatory variables ($p < 0.005$, $F = 8.71$, and $p < 0.01$, $F = 4.46$, respectively) accounting for the
438 variation of MicroResp soil metabolic diversity (Fig. 6B). The total nitrogen concentration showed negative
439 relationships with Shannon diversity (H') and Pielou's evenness (J) indices, confirmed by significant Pearson
440 linear correlations ($p = 1.50 \times 10^{-4}$, $r = -0.92$, and $p = 3.08 \times 10^{-3}$, $r = 0.83$, respectively). The metal pollution
441 index and the total nitrogen concentration were the strongest determinants of both axes (Fig. 6C) and had a
442 significant effect on Biolog metabolic diversity indices ($p < 0.01$, $F = 7.77$, and $p < 0.05$, $F = 4.71$, respectively).
443 The metal pollution index showed a negative relationship with metabolic richness and Shannon diversity index
444 (H') confirmed by slightly significant negative linear correlations ($p = 0.06$, $r = -0.61$ for both of them). Total
445 nitrogen exhibited a negative relationship with Pielou's evenness index (J), confirmed by a significant linear
446 correlation ($p = 0.02$, $r = -0.73$).

Discussion

We studied ten different soils presenting metal and/or PAH pollution gradients and exhibiting a wide range of anthropisation levels. Although the ten soils came from various sites with different types and levels of plant colonization, they mostly clustered in three groups based on their physico-chemical properties and pollution levels. These three groups reflected their use, whether industrial or low anthropised. Settling pond soils were highly polluted with MTEs, with higher contents of total organic carbon and nitrogen and a siltier texture than the soils from the other groups. Slag heap soils were the sandiest and the most PAH-polluted soils, and also exhibited middle-high metal pollution: mostly MTEs for sh-Te, sh-NM, and sh-Ho, while sh-Uc contained a very high iron concentration. The control soils were the least metal- and PAH-polluted ones; they were also the most clayey soils, and had the highest dissolved organic carbon and potassium contents. Apart from the identification of well known edaphic factors impacting the microbial diversity, we also aimed at identifying the impact of pollutants on the microbial community composition. The taxonomic and metabolic functional diversity of the microbial communities inhabiting the ten soils was characterized. We studied bacterial taxonomic diversity based on 16S rRNA gene sequencing, and functional diversity based on measurements of the utilisation of various carbon substrates involved in different functions to estimate the impact of land use on microbial community diversity and functions. We focused on functions related to the carbon cycle, one of the most important biogeochemical cycles for soil functioning [54, 55]. Although the taxonomic and functional diversity of soil microorganisms is extensively studied to better understand ecosystem functioning, the real link between taxon occurrence and functional richness remains poorly understood in most ecosystems [56], particularly for microbial communities. Various authors suggest that the functions related to carbon mineralisation are redundant [57, 58]. Besides, the loss of species or the modification of microbial community composition does not necessarily induce a loss of functions. In order to better understand the effect of pollution on microbial communities, it is thus important to study both taxonomic and functional diversity, using a combination of tools.

One of the objectives of this study was to identify soil parameters mostly shaping microbial community diversity in the ten soils. Although, some of the measured diversity indicators seemed constant in all soils, our data revealed that both pollutant and physico-chemical parameters strongly affected part of the taxonomic and functional structures.

Non-impacted microbial parameters

We noted few variations in bacterial community composition among our soils, with all the major phyla present in each soil, and no phylum significantly dominant or under-represented in highly anthropised soils. The taxonomic diversity indices of the polluted soils were not significantly different from those of the control soils. Previous studies reported similar trends with no difference among the bacterial taxonomic diversity indices of historically mining-impacted *vs.* unpolluted sediments [59]. Indeed, long-term adaptation and resilience [60] of the bacterial communities, being as diverse as in control soil [22] or over a metal polluted gradient [61], was

previously observed. Additionally, except for sp-RM that exhibited a very strong decrease of metabolic richness, at least one substrate from each carbon substrate guild from Biolog plates was utilised by each soil. In some cases, metabolic potentials were not affected by metal pollution as shown in three forest soils gradually polluted by Zn and Cd [62]. The differences of substrate-induced respiration observed among soils were less pronounced using the MicroResp than the Biolog method, and were essentially linked to the soil basal respiration rates as previously observed [63]. Contrarily to many studies [63, 64, 65], basal respiration rates and substrate-induced respiration were mostly not affected by pollution (metals and PAH) level. Additionally to the bacterial activity, MicroResp can also integrate fungal respiration. Although, fungi are major actors of the carbon cycle [66], their relative abundances (ratio between 18S and 16S rDNA copy numbers) were not correlated with the respiration rates because the three soil groups had similar fungal density (18S rDNA copies.g^{-1} dw soil). Moreover, even if fungi harbor high metal tolerance [67] no link between fungal abundances, respiration rates and soil pollution was highlighted.

Impact of metals on microbial diversity

The relative toxicity of a pollutant depends more on its available content than on its total content. The bioavailability of MTEs in these soils was relatively low since most of them had a pH value above 7. Only soil He with a pH of 5.4 had a relatively higher MTE availability than the other soils of the same group, although it was not contaminated. Except for this soil, using the relative metal pollution index or the available fraction of MTEs such as Zn showed the same tendency, that is why we mainly used the former to compare the soils.

The metal pollution index and/or the total zinc content were positively correlated with the relative proportion of unclassified OTUs and Gemmatimonadetes and Chloroflexi phyla (correlation with available Zinc content have p value of 0.077, 0.088 and 0.120, respectively). Unclassified OTUs may represent extensive unexplored bacterial diversity that may have original properties allowing them to survive and grow in strongly metal-contaminated environments. Gemmatimonadetes are commonly found in heavy-metal contaminated soils [68]. A positive relationship between the relative proportion of Gemmatimonadetes or Chloroflexi and metal pollution was shown in lake sediment historically polluted with zinc and lead [69] and in the soil of an abandoned Pb-Zn mine [70]. The Chloroflexi group is known to have a high stress tolerance ability [71], which could explain its development in our metal-polluted soils. At the OTU level, a few OTUs were positively correlated to the metal pollution index, and these OTUs were also positively correlated to the P and N contents. These OTUs were affiliated to Actinobacteria members, closely related to the AKIW543 clone, the *Acidimicrobineae* and *Aeromicrobium* genera, and to Firmicutes affiliated to the *Bacillus* genus. Very little information is available about the two former but few strains belonging to *Aeromicrobium* and *Bacillus* genera have already been isolated from former mining sites [72] and from heavy-metal contaminated soil [73].

The metal pollution index and/or the total and available zinc contents were negatively correlated to the richness and diversity of the substrates utilised in Biolog plates, suggesting that functional diversity (number of metabolic functions) was reduced in metal-polluted soils [74]. Similarly, when comparing soils sampled at different distances from a site historically metal-polluted with As, Cu, and Pb, Boshoff et al. [29] found lower

functional diversity in the soils closest to the contamination source. It may result from the replacement of sensitive species by more resistant ones having different and less versatile metabolic properties [75] maybe due to an energy cost balance between metal stress survival mechanisms and substrate utilisation efficiency [76]. Functional diversity may indicate the capacity of the community to adapt its metabolism, relative composition, and size to various changes in environmental conditions [77]. In our study, the low metabolic richness of the bacterial community in the metal-polluted soils may have disturbed carbon recycling and soil functioning.

Additionally, using Biolog for tolerance tests, lower zinc sensitivity (or higher tolerance) of the bacterial community inhabiting high metal-contaminated soils was shown as compared to low-polluted or unpolluted soils, suggesting an adaptation of communities to metal stress, as previously observed [78]. It is well accepted that microorganisms coming from highly polluted environments are more tolerant to pollution than those coming from less polluted environments [21].

Among our soil collection, sh-Uc had the highest iron concentration and relatively low concentrations of other metals, resulting in a middle-high metal pollution index. This soil had similar taxonomic but slightly higher functional diversity indices as compared to other soils presenting a middle-high metal pollution index. Unlike other metals such as Cd or Pb, Fe is an essential element for almost all living organisms and is involved in numerous metabolic processes. Moreover, due to its extremely high total concentration in sh-Uc, iron was probably mostly present as insoluble oxides and unavailable forms. This finding suggests that although iron was present in a very high total concentration in sh-Uc, it had a lower effect on microbial diversity than other metals such as Zn, Cd, or Pb.

Impact of PAH on microbial diversity

We highlighted various correlations between PAH pollution and the proportions of some phyla or OTU abundance, but found no relationship with functional metabolic diversity, suggesting a limited impact of PAH on microbial community carbon-cycle related functions in our soils. Total and available PAH contents were both positively correlated to the proportions of Proteobacteria (mostly Gamma-Proteobacteria) and Nitrospirae phyla, even if in the literature the Nitrospirae phylum seemed to be negatively impacted by PAH content and bioavailability [79]. Proteobacteria and Gamma-Proteobacteria were previously found in greater proportions in pyrene-amended soil [80] and can be involved in PAH degradation [81]. The abundance of some OTUs was also positively correlated to the total PAH pollution level, but was not affected by all other soil parameters, suggesting an advantage conferred in the presence of PAHs. Most of them were found predominant in PAH-polluted environments, i.e. bacteria belonging to *Flavobacterium* [82], *Flexibacter* [83], *Sphingomonadaceae* [84] and Chloroflexi [85] were detected or isolated from PAH-contaminated soils. Firstly, PAH pollution could have contributed to shape bacterial communities by favouring species able to metabolise PAHs. Secondly, in our soils, due to ageing, available PAH concentrations were low as compared to total concentrations and did not negatively affect taxonomic or functional diversity at the community level, indicating no major toxicity impact of PAHs on bacterial diversity.

Impact of physico-chemical parameters on microbial diversity

Apart from the soil pollutants, microbial communities can be affected by physico-chemical parameters. It is well known that the pH is one of the major parameters that shapes microbial community composition [30, 86]. Except one control soil (ctrl-He), our soils were chosen with a similar slightly alkaline pH to avoid a too high influence of this parameter that could have hidden the structuring impact of other parameters. Thus, the pH has little impact on taxonomic and functional diversity, although the proportions of few OTUs mostly affiliated to Verrucomicrobial DA101 members and commonly found as dominant bacteria in soils [87] increased when the pH decreased.

The soil texture, and especially the sand fraction proportion, was the strongest determinant of bacterial taxonomic diversity in our soils, but no link with metabolic functional diversity was highlighted. The relative proportion of the soil sandy fraction was indeed positively correlated with taxonomic richness, evenness, and Shannon diversity indices, and the relative proportion of Alpha-Proteobacteria [88], whereas the relative proportions of silt and clay negatively influenced the richness and evenness indices. Fine-textured soil can protect microbes from predation by protozoans, reduce variations in water availability, and maintain higher microbial abundance [89]. Conversely, coarse-textured soils allow for a better aeration and water circulation providing various microhabitats and supporting growth of diverse microorganisms adapted to limited nutrient conditions or able to use a wider range of substrates [88]. Similarly to our results, Chau et al. [90] found a positive linear relationship between sand content and taxonomic richness, while Kandeler et al. [91] found that the small-size fraction promoted bacterial diversity. These contradictory results could be related to soil fractionation techniques [90], as we based textures on particle granulometry, not on mineralogy (i.e. the sandy fraction could contain sand but also other particles). Finally, the texture may affect pollutant availability, which could indirectly affect microbial diversity.

While the soil total organic carbon content was not the main parameter explaining taxonomic diversity, it was negatively correlated to the functional diversity indices, calculated from MicroResp and Biolog data, to the utilisation level of 6 substrates (phthalic, ferulic, succinic, and aconitic acids, Tween 40, and phenylethylamine), and to the number of polymer, carboxylic acid and miscellaneous substrates utilised in Biolog microtiter plates. We noticed that in the redundancy analysis, the total organic carbon content co-varied with the metal pollution index, as previously shown by Valsecchi et al. [92] on a collection of 16 soils. As explained above, metal pollution may have reduced the functional capacities of the microbial community. The resulting lower microbial functional diversity and activity may have reduced organic carbon recycling in the soils, resulting in an accumulation of total organic carbon and organic matter. Similarly, rates of organic matter (i.e. litter or plant polymer such as cellulose) degradation were lower in metal-contaminated than unpolluted soils [93, 94]. This finding could be explained by a decrease of enzymatic activities involved in the C cycle in metal-polluted soils [91]. Moreover, Lucisine et al. [95] also explained that accumulation of organic matter at the surface of brownfield soil could be partly due to the lack of endogenous metal-sensitive earthworm species limiting organic matter incorporation in the deeper soil layers.

595 We observed that the total nitrogen content was positively correlated with soil basal respiration, with ribose-,
596 pyruvate-, and asparagine-induced respiration, and with 16S rRNA gene copy numbers. These relationships
597 suggest that in some of our soils, nitrogen present in very low concentrations was one of the limiting factors of
598 microbial growth and activity. N limitation can indeed occur in some cases depending on the quality of the
599 available carbon substrate [96, 97]. Additionally, the relative proportions of the Actinobacteria phylum and of a
600 few OTUs affiliated to Actinobacteria and Firmicutes were positively correlated to the total nitrogen content.
601 As discussed above, these OTUs were also positively correlated to the metal pollution index indicating a
602 simultaneous influence of various soil parameters on microbial community composition. As explained for total
603 organic carbon, metal pollution partly inhibits soil enzyme activities and organic matter decomposition [98], so
604 that the total nitrogen content potentially increases in the most polluted soils. Moreover, several strains of
605 Bacilli isolated from soils are known as nitrogen-fixing bacteria [99] and could contribute to increase the
606 nitrogen content. On the contrary, Bacteroidetes phyla and a few OTUs affiliated to Acidobacteria were
607 negatively correlated with the total nitrogen content. Acidobacteria are often classified as oligotrophs [100],
608 which are favoured in nutrient-poor environments. Moreover, a negative relationship between the total
609 nitrogen content and the functional evenness index was mostly explained by a higher mineralising activity in a
610 few substrates. Nitrogen may have impacted bacterial community composition, favouring the development of
611 certain species with higher metabolic activity for certain specific substrates.
612

613 ## Conclusions

614

615 We studied a collection of 10 soils presenting different anthropisation levels. Based on their physico-chemical
616 characteristics and on metal and PAH pollution levels, these soils were gathered in 3 groups corresponding to
617 their use, i.e. either industrial (slag heap and settling pond) or low anthropised (control soil). Although
618 taxonomic diversity largely varied among soils, the occurrence of a few bacterial phyla and OTUs was
619 influenced by metal and PAH pollution as well as by the pH, texture, and the total N content. Furthermore,
620 metal pollution, particularly zinc concentrations, seems to have selected more metal-tolerant communities but
621 with reduced metabolic functional diversity and activity. Apart from metal pollution, the N content appeared to
622 be one of the main factors limiting microbial activity in our soils. These reduced activity and metabolic
623 functional diversity may have contributed to an accumulation of organic matter in the most metal-polluted
624 soils. Considering all abiotic and biotic soil characteristics, especially metabolic functional diversity, we are now
625 able to rank our soils based on their impact on microbial communities (i.e. control soils have the lowest effect,
626 while settling pond soils have the highest). Although it would be very interesting to study a wider range of soil
627 to draw more generalizable conclusions, the study of 10 soils already allowed us to identify the drivers of
628 microbial diversity at both the taxonomic and functional level.

629

630

Acknowledgements

We would like to thank Arcelor Mittal, EPFL, GISFI, ONF, and LTO of Montiers (ANDRA/INRA, M.P. Turpault and S. Uroz) for giving us access to the different sampling sites. We would like to thank G. Kitzinger and D. Billet (LIEC, Nancy, France) as well as J. Marchand (PTEF, INRA Champenoux, France) for technical assistance and A. Meyer (LIEC, Metz, France) for statistical analysis support. Fundings: This study was supported by the Agence Nationale de la Recherche (RhizOrg project ANR-13-JSV7-000701), the French national program EC2CO-(EcobioS project) and the OSU-OteLo (TraitMic project).

Figure captions

Table 1 | Physico-chemical characteristics of the ten soils. *Parameters were measured one time on one mean sample. For soil groups, values are means (n=3 for ctrl and sp soils, and n=4 for sh soil) ± standard error of the mean. Significant results of Kruskal-Wallis tests (p < 0.05), testing differences among the 3 soil groups, are indicated by different letters, and no letter appears when non-significant differences were found. For statistical analyses, values lower than the detection limits of the method were replaced by 1, except for available phosphorus for which the value was replaced by 0.05. The metals used for calculating the metal pollution index (Mi) are indicated by a star. Abbreviations of soil names and groups: Di: Dieulouard, Ho: Homécourt, He: Hémilly, MsM: Mont St Martin, Mo: Montiers, RM: Russange-Micheville, NM: Neuves Maisons, Po: Pompey, Te: Terville, Uc: Uckange; ctrl: control, sh: slag heap, sp: settling pond. Abbreviations of soil characteristics: PAH: polycyclic aromatic hydrocarbons, CEC: cation exchange capacity.*

Table 2 | Microbial, taxonomic and functional characteristics of the ten soils. *Values are means (n = 3 or 4) ± standard error of the mean. For soil groups, values are means (n=3 for ctrl and sp soils, and n=4 for sh soil) ± standard error of the mean. Significant results of Kruskal-Wallis tests (p < 0.05), testing differences among the 3 soil groups, are indicated by different letters, and no letter appears when non-significant differences were found.*

Figure 1 | Principal Component Analysis (PCA) and correlation circle based on the physico-chemical, pollution, and texture characteristics of the ten soils. *On the PCA: Soils (Di: Dieulouard, Ho: Homécourt, He: Hémilly, MsM: Mont St Martin, Mo: Montiers, RM: Russange-Micheville, NM: Neuves Maisons, Po: Pompey, Te: Terville, Uc: Uckange) were grouped in three types according to their industrial history (sp: settling pond; sh: slag heap; ctrl: control). On the correlation circle: N: total nitrogen; C_org: total organic carbon; P_Olsen: available phosphorus; Mi: metal pollution index; PAH: sum of 16 regulatory PAHs; K_t: total potassium; sand and clay: proportions of the sand and clay fractions, respectively.*

Figure 2 | Taxonomic composition of the bacterial communities of the ten soil samples. V*alues are means (n = 3), and error-bars represent standard errors of the mean for each soil. The group named Others included OTUs affiliated to the following phyla: BD1-5, Chlamydiae, Chlorobi, Cyanobacteria, Deinococcus-Thermus, Fusobacteria, Spirochaetes, WCHB1-60, Synergistetes, and Candidate divisions BRC1, OD1, OP10, SR1, TG-1, TM6, WS3, and WS6. Statistical differences among phylum proportions in the soil groups are indicated by different letters (Kruskal-Wallis test, p < 0.05).*

672 **Figure 3 | Cumulated substrate-induced respiration (SIR) in the presence of six carbon sources, and basal soil**
673 **respiration measured using the MicroResp method.** *Values are means (n = 4 for SIR and n = 8 for basal*
674 *respiration), and error bars represent standard errors of the mean for each soil. Statistical differences among*
675 *the soil groups are indicated by different letters (Kruskal-Wallis test, p < 0.05).*

676

677 **Figure 4 | Catabolic richness and average well color development (AWCD) measured after 96h of incubation**
678 **using Biolog microtiter plates.** Values are means *(n = 3),* and error bars represent standard errors of the mean
679 for each soil. *Sixty-two carbon sources were tested: 4 PAHs, 6 aromatic acids, 9 amino acids, 7 polymers, 14*
680 *carbohydrates, 17 carboxylic acids, and 5 miscellaneous (for details see Supplemental Table S1). Statistical*
681 *differences among the soil groups are indicated by different letters (Kruskal-Wallis test, p > 0.05). As none of the*
682 *PAH compounds was significantly degraded, they were excluded from the statistical analysis.*

683

684 **Figure 5 | Linear regression between the inhibition rate of carbon substrate utilisation measured using**
685 **Biolog microtiter plates (n = 3) with and without zinc addition, and available zinc concentrations in the ten**
686 **soils.** *The blue line represents the linear model of regression (y = -0.0006x + 60.98; where y is the inhibition rate*
687 *and x is the available zinc content of the soil). The dark grey area represents the confidence interval, and the*
688 *light grey area represents the prediction interval (95%). Settling pond, slag heap, and control soils are*
689 *represented by red, green, and blue dots, respectively.*

690

691 **Figure 6 | Redundancy analysis (RDA) of soil bacterial community diversity (A), MicroResp soil catabolic**
692 **diversity (B), and Biolog catabolic diversity (C), each of them constrained by soil environmental**
693 **characteristics.**

694 *For each RDA, the explanatory variables that best explained the variation of diversity indices (response*
695 *variables) were selected by backward selection. Explanatory and response variables are in red and black,*
696 *respectively. Abbreviations of explanatory variables: N: total nitrogen; C_org: total organic carbon; Mi: metal*
697 *pollution index; PAH: sum of 16 regulatory PAHs; K_t: total potassium; sand: proportion of the sandy fraction.*
698 *Abbreviations of response variables: S: richness; Chao1: extrapolated richness; H: Shannon's diversity index; J:*
699 *Pielou's evenness index; 16S: index for bacterial taxonomic diversity. MR: index for MicroResp soil catabolic*
700 *diversity. BLG: index for Biolog catabolic diversity. Abbreviations for soils: Di: Dieulouard, Ho: Homécourt, He:*
701 *Hémilly, MsM: Mont St Martin, Mo: Montiers, RM: Russange-Micheville, NM: Neuves Maisons, Po: Pompey, Te:*
702 *Terville, Uc: Uckange). Soils were grouped in three types according to their history (sp: settling pond; sh: slag*
703 *heap; ctrl: control). The p values and F coefficients, for axes and soil properties, are provided in the*
704 *supplemental Table S2.*

705

Supplemental material

Table S1 | Substrates used in the Biolog and MicroResp experiments.

Table S2 | The p values and F coefficients for axes and soil properties for the redundancy analyses presented on the Figure 6.

Figure S1 | Heatmap based on the similarity matrix obtained from the PLSr analysis (implemented using 5 components). *The heatmap depicts the positive (red) and negative (blue) correlations between OTU abundances (the predictor matrix) and the soil physico-chemical properties (the response variables) investigated in this study. Dendrograms indicate the level of similarity among the clusters present in the heatmap. The hierarchical clustering was based on the Euclidean distance and the complete linkage method.*

References

1. (2016) BASOL. http://basol.developpement-durable.gouv.fr/. Accessed 11 Sep 2017

2. Rachwał M, Magiera T, Wawer M (2015) Coke industry and steel metallurgy as the source of soil contamination by technogenic magnetic particles, heavy metals and polycyclic aromatic hydrocarbons. Chemosphere 138:863–873. doi: 10.1016/j.chemosphere.2014.11.077

3. Joimel S, Cortet J, Jolivet CC, et al (2016) Physico-chemical characteristics of topsoil for contrasted forest, agricultural, urban and industrial land uses in France. Sci Total Environ 545:40–47. doi: 10.1016/j.scitotenv.2015.12.035

4. Wilcke W (2000) SYNOPSIS Polycyclic Aromatic Hydrocarbons (PAHs) in Soil — a Review. J Plant Nutr Soil Sci 163:229–248. doi: 10.1002/1522-2624(200006)163:3<229::AID-JPLN229>3.0.CO;2-6

5. Dhelft P (1994) Épuration du gaz de haut fourneau. Tech L'ingénieur Métaux Ferr Élabor Métal Prim TIB366DUO. (ref. article : m7422)

6. Johnsen AR, Wick LY, Harms H (2005) Principles of microbial PAH-degradation in soil. Environ Pollut 133:71–84. doi: 10.1016/j.envpol.2004.04.015

7. Janssen CR, Heijerick DG, De Schamphelaere KAC, Allen HE (2003) Environmental risk assessment of metals: tools for incorporating bioavailability. Environ Int 28:793–800. doi: 10.1016/S0160-4120(02)00126-5

8. Kim R-Y, Yoon J-K, Kim T-S, et al (2015) Bioavailability of heavy metals in soils: definitions and practical implementation--a critical review. Environ Geochem Health 37:1041–1061. doi: 10.1007/s10653-015-9695-y

9. Cerniglia CE (1992) Biodegradation of polycyclic aromatic hydrocarbons. Biodegradation 3:351–368. doi: 10.1007/BF00129093

10. Hatzinger PB, Alexander M (1995) Effect of aging of chemicals in soil on their biodegradability and extractability. Environ Sci Technol 29:537–545. doi: 10.1021/es00002a033

11. Cébron A, Faure P, Lorgeoux C, et al (2013) Experimental increase in availability of a PAH complex organic contamination from an aged contaminated soil: consequences on biodegradation. Environ Pollut Barking Essex 1987 177:98–105. doi: 10.1016/j.envpol.2013.01.043

12. Abdu N, Abdullahi AA, Abdulkadir A (2017) Heavy metals and soil microbes. Environ Chem Lett 15:65–84. doi: 10.1007/s10311-016-0587-x

13. Andreoni V, Cavalca L, Rao MA, et al (2004) Bacterial communities and enzyme activities of PAHs polluted soils. Chemosphere 57:401–412. doi: 10.1016/j.chemosphere.2004.06.013

14. Grant RJ, Muckian LM, Clipson NJW, Doyle EM (2007) Microbial community changes during the bioremediation of creosote-contaminated soil. Lett Appl Microbiol 44:293–300. doi: 10.1111/j.1472-765X.2006.02066.x

15. Sawulski P, Clipson N, Doyle E (2014) Effects of polycyclic aromatic hydrocarbons on microbial community structure and PAH ring hydroxylating dioxygenase gene abundance in soil. Biodegradation 25:835–847. doi: 10.1007/s10532-014-9703-4

16. Sutton NB, Maphosa F, Morillo JA, et al (2013) Impact of long-term diesel contamination on soil microbial community structure. Appl Environ Microbiol 79:619–630. doi: 10.1128/AEM.02747-12

17. Kelly JJ, Häggblom M, Tate RL (1999) Changes in soil microbial communities over time resulting from one time application of zinc: a laboratory microcosm study. Soil Biol Biochem 31:1455–1465. doi: 10.1016/S0038-0717(99)00059-0

18. Moffett BF, Nicholson FA, Uwakwe NC, et al (2003) Zinc contamination decreases the bacterial diversity of agricultural soil. FEMS Microbiol Ecol 43:13–19. doi: 10.1111/j.1574-6941.2003.tb01041.x

19. Cébron A, Norini M-P, Beguiristain T, Leyval C (2008) Real-Time PCR quantification of PAH-ring hydroxylating dioxygenase (PAH-RHDα) genes from Gram positive and Gram negative bacteria in soil and sediment samples. J Microbiol Methods 73:148–159. doi: 10.1016/j.mimet.2008.01.009

20. Diaz-Ravina M, Baath E (1996) Development of Metal Tolerance in Soil Bacterial Communities Exposed to Experimentally Increased Metal Levels. Appl Environ Microbiol 62:2970–2977.

21. Blanck H (2002) A Critical Review of Procedures and Approaches Used for Assessing Pollution-Induced Community Tolerance (PICT) in Biotic Communities. Hum Ecol Risk Assess Int J 8:1003–1034 . doi: 10.1080/1080-700291905792

22. Bourceret A, Cébron A, Tisserant E, et al (2016) The Bacterial and Fungal Diversity of an Aged PAH- and Heavy Metal-Contaminated Soil is Affected by Plant Cover and Edaphic Parameters. Microb Ecol 71:711–724. doi: 10.1007/s00248-015-0682-8

23. Lindgren JF, Hassellöv I-M, Nyholm JR, et al (2017) Induced tolerance in situ to chronically PAH exposed ammonium oxidizers. Mar Pollut Bull 120:333–339. doi: 10.1016/j.marpolbul.2017.05.044

24. Thavamani P, Malik S, Beer M, et al (2012) Microbial activity and diversity in long-term mixed contaminated soils with respect to polyaromatic hydrocarbons and heavy metals. J Environ Manage 99:10–17. doi: 10.1016/j.jenvman.2011.12.030

25. Lu M, Xu K, Chen J (2013) Effect of pyrene and cadmium on microbial activity and community structure in soil. Chemosphere 91:491–497. doi: 10.1016/j.chemosphere.2012.12.009

26. Markowicz A, Cycon M, Piotrowska-Seget Z (2016) Microbial Community Structure and Diversity in Long-term Hydrocarbon and Heavy Metal Contaminated Soils. Int J Environ Res 10:321–332. doi: 10.22059/ijer.2016.57792

27. Zak JC, Willig MR, Moorhead DL, Wildman HG (1994) Functional diversity of microbial communities: A quantitative approach. Soil Biol Biochem 26:1101–1108. doi: 10.1016/0038-0717(94)90131-7

28. Campbell CD, Chapman SJ, Cameron CM, et al (2003) A rapid microtiter plate method to measure carbon dioxide evolved from carbon substrate amendments so as to determine the

physiological profiles of soil microbial communities by using whole soil. Appl Environ Microbiol 69:3593–3599

29. Boshoff M, De Jonge M, Dardenne F, et al (2014) The impact of metal pollution on soil faunal and microbial activity in two grassland ecosystems. Environ Res 134:169–180. doi: 10.1016/j.envres.2014.06.024

30. Fierer N, Jackson RB (2006) The diversity and biogeography of soil bacterial communities. Proc Natl Acad Sci 103:626–631. doi: 10.1073/pnas.0507535103

31. Nacke H, Thürmer A, Wollherr A, et al (2011) Pyrosequencing-based assessment of bacterial community structure along different management types in German forest and grassland soils. PloS One 6:e17000. doi: 10.1371/journal.pone.0017000

32. Bissett A, Richardson AE, Baker G, Thrall PH (2011) Long-term land use effects on soil microbial community structure and function. Appl Soil Ecol 51:66–78. doi: 10.1016/j.apsoil.2011.08.010

33. Baize D (2000) Teneurs totales en « métaux lourds » dans les sols français : résultats généraux du programme ASPITET. Courr Environ Inra 39.

34. Cennerazzo J, de Junet A, Audinot J-N, Leyval C (2017) Dynamics of PAHs and derived organic compounds in a soil-plant mesocosm spiked with 13C-phenanthrene. Chemosphere 168:1619–1627. doi: 10.1016/j.chemosphere.2016.11.145

35. Reid BJ, Stokes JD, Jones KC, Semple KT (2000) Nonexhaustive Cyclodextrin-Based Extraction Technique for the Evaluation of PAH Bioavailability. Environ Sci Technol 34:3174–3179. doi: 10.1021/es990946c

36. Jones DL, Willett VB (2006) Experimental evaluation of methods to quantify dissolved organic nitrogen (DON) and dissolved organic carbon (DOC) in soil. Soil Biol Biochem 38:991–999. doi: 10.1016/j.soilbio.2005.08.012

37. Thomas F, Cébron A (2016) Short-Term Rhizosphere Effect on Available Carbon Sources, Phenanthrene Degradation, and Active Microbiome in an Aged-Contaminated Industrial Soil. Syst Microbiol 92. doi: 10.3389/fmicb.2016.00092

38. Lueders T, Wagner B, Claus P, Friedrich MW (2004) Stable isotope probing of rRNA and DNA reveals a dynamic methylotroph community and trophic interactions with fungi and protozoa in oxic rice field soil. Environ Microbiol 6:60–72. doi: 10.1046/j.1462-2920.2003.00535.x

39. Felske A, Akkermans ADL, Vos WMD (1998) Quantification of 16S rRNAs in Complex Bacterial Communities by Multiple Competitive Reverse Transcription-PCR in Temperature Gradient Gel Electrophoresis Fingerprints. Appl Environ Microbiol 64:4581–4587.

40. Cébron A, Beguiristain T, Bongoua-Devisme J, et al (2015) Impact of clay mineral, wood sawdust or root organic matter on the bacterial and fungal community structures in two aged PAH-contaminated soils. Environ Sci Pollut Res Int 22:13724–13738. doi: 10.1007/s11356-015-4117-3

41. Thion C, Cebron A, Beguiristain T, Leyval C (2012) Long-term in situ dynamics of the fungal communities in a multi-contaminated soil are mainly driven by plants. Fems Microbiol Ecol 82:169–181. doi: 10.1111/j.1574-6941.2012.01414.x

42. Muyzer G, de Waal EC, Uitterlinden AG (1993) Profiling of complex microbial populations by denaturing gradient gel electrophoresis analysis of polymerase chain reaction-amplified genes coding for 16S rRNA. Appl Environ Microbiol 59:695–700.

43. Caporaso JG, Lauber CL, Walters WA, et al (2011) Global patterns of 16S rRNA diversity at a depth of millions of sequences per sample. Proc Natl Acad Sci U S A 108 Suppl 1:4516–4522. doi: 10.1073/pnas.1000080107

44. Kozich JJ, Westcott SL, Baxter NT, et al (2013) Development of a Dual-Index Sequencing Strategy and Curation Pipeline for Analyzing Amplicon Sequence Data on the MiSeq Illumina Sequencing Platform. Appl Environ Microbiol 79:5112–5120. doi: 10.1128/AEM.01043-13

45. Schloss PD, Westcott SL, Ryabin T, et al (2009) Introducing mothur: Open-Source, Platform-Independent, Community-Supported Software for Describing and Comparing Microbial Communities. Appl Environ Microbiol 75:7537–7541. doi: 10.1128/AEM.01541-09

46. Edgar RC, Haas BJ, Clemente JC, et al (2011) UCHIME improves sensitivity and speed of chimera detection. Bioinforma Oxf Engl 27:2194–2200. doi: 10.1093/bioinformatics/btr381

47. Hill TCJ, Walsh KA, Harris JA, Moffett BF (2003) Using ecological diversity measures with bacterial communities. FEMS Microbiol Ecol 43:1–11. doi: 10.1111/j.1574-6941.2003.tb01040.x

48. Oksanen J, Blanchet FG, Friendly M, et al (2017) vegan: Community Ecology Package. R package version 1.17-2. *R Development Core Team. R: A language and environment for statistical computing. Vienna: R Foundation for Statistical Computing*.

49. Dray S, Dufour A-B (2007) The ade4 Package: Implementing the Duality Diagram for Ecologists. J Stat Softw 22:1–20. doi: 10.18637/jss.v022.i04

50. Wold S, Ruhe A, Wold H, Dunn I W (1984) The Collinearity Problem in Linear Regression. The Partial Least Squares (PLS) Approach to Generalized Inverses. SIAM J Sci Stat Comput 5:735–743. doi: 10.1137/0905052

51. Wold S, Sjöström M, Eriksson L (2001) PLS-regression: a basic tool of chemometrics. Chemom Intell Lab Syst 58:109–130. doi: 10.1016/S0169-7439(01)00155-1

52. Lê Cao KA, Rohart F, Gonzalez I, et al (2017) mixOmics: Omics Data Integration Project. Available from: https://CRAN.R-project.org/package=mixOmics.

53. Rohart F, Gautier B, Singh A, Cao K-AL (2017) mixOmics: An R package for 'omics feature selection and multiple data integration. PLOS Comput Biol 13:e1005752. doi: 10.1371/journal.pcbi.1005752

54. Nielsen UN, Ayres E, Wall DH, Bardgett RD (2011) Soil biodiversity and carbon cycling: a review and synthesis of studies examining diversity–function relationships. Eur J Soil Sci 62:105–116. doi: 10.1111/j.1365-2389.2010.01314.x

55. Schimel JP, Schaeffer SM (2012) Microbial control over carbon cycling in soil. Front Microbiol 3:348. doi: 10.3389/fmicb.2012.00348

56. Nannipieri P, Ascher J, Ceccherini MT, et al (2003) Microbial diversity and soil functions. Eur J Soil Sci 54:655–670. doi: 10.1046/j.1351-0754.2003.0556.x

874 57. Yin B, Crowley D, Sparovek G, et al (2000) Bacterial Functional Redundancy along a Soil
875 Reclamation Gradient. Appl Environ Microbiol 66:4361–4365. doi: 10.1128/AEM.66.10.4361-
876 4365.2000

877 58. Rousk J, Brookes PC, Bååth E (2009) Contrasting Soil pH Effects on Fungal and Bacterial
878 Growth Suggest Functional Redundancy in Carbon Mineralization. Appl Environ Microbiol
879 75:1589–1596. doi: 10.1128/AEM.02775-08

880 59. Reis MP, Barbosa FAR, Chartone-Souza E, Nascimento AMA (2013) The prokaryotic community
881 of a historically mining-impacted tropical stream sediment is as diverse as that from a pristine
882 stream sediment. Extremophiles 17:301–309 . doi: 10.1007/s00792-013-0517-9

883 60. Gillan DC, Danis B, Pernet P, et al (2005) Structure of sediment-associated microbial
884 communities along a heavy-metal contamination gradient in the marine environment. Appl
885 Environ Microbiol 71:679–690. doi: 10.1128/AEM.71.2.679-690.2005

886 61. Azarbad H, Niklińska M, Laskowski R, et al (2015) Microbial community composition and
887 functions are resilient to metal pollution along two forest soil gradients. FEMS Microbiol Ecol
888 91:1–11. doi: 10.1093/femsec/fiu003

889 62. Niklińska M, Chodak M, Stefanowicz A (2004) Community level physiological profiles of
890 microbial communities from forest humus polluted with different amounts of Zn, Pb, and Cd—
891 Preliminary study with BIOLOG ecoplates. Soil Sci Plant Nutr 50:941–944 . doi:
892 10.1080/00380768.2004.10408558

893 63. Nordgren A, Bååth E, Söderström B (1988) Evaluation of soil respiration characteristics to
894 assess heavy metal effects on soil microorganisms using glutamic acid as a substrate. Soil Biol
895 Biochem 20:949–954. doi: 10.1016/0038-0717(88)90109-5

896 64. Bérard A, Capowiez L, Mombo S, et al (2016) Soil microbial respiration and PICT responses to
897 an industrial and historic lead pollution: a field study. Environ Sci Pollut Res 23:4271–4281.
898 doi: 10.1007/s11356-015-5089-z

899 65. Stazi SR, Moscatelli MC, Papp R, et al (2017) A Multi-biological Assay Approach to Assess
900 Microbial Diversity in Arsenic (As) Contaminated Soils. Geomicrobiol J 34:183–192. doi:
901 10.1080/01490451.2016.1189015

902 66. Bardgett RD, Freeman C, Ostle NJ (2008) Microbial contributions to climate change through
903 carbon cycle feedbacks. The ISME journal, 2(8), 805.

904 67. Rajapaksha RMCP, Tobor-Kapłon MA, Bååth E (2004). Metal toxicity affects fungal and
905 bacterial activities in soil differently. Applied and Environmental Microbiology, 70(5), 2966-
906 2973. doi: 10.1128/AEM.70.5.2966-2973.2004

907 68. Sullivan TS, McBride MB, Thies JE (2013) Rhizosphere microbial community and Zn uptake by
908 willow (Salix purpurea L.) depend on soil sulfur concentrations in metalliferous peat soils. Appl
909 Soil Ecol 67:53–60. doi: 10.1016/j.apsoil.2013.02.003

910 69. Ni C, Horton DJ, Rui J, et al (2016) High concentrations of bioavailable heavy metals impact
911 freshwater sediment microbial communities. Ann Microbiol 66:1003–1012. doi:
912 10.1007/s13213-015-1189-8

70. Epelde L, Lanzén A, Blanco F, et al (2015) Adaptation of soil microbial community structure and function to chronic metal contamination at an abandoned Pb-Zn mine. FEMS Microbiol Ecol 91:1–11. doi: 10.1093/femsec/fiu007

71. Fierer N (2017) Embracing the unknown: disentangling the complexities of the soil microbiome. Nat Rev Microbiol 15:579–590. doi: 10.1038/nrmicro.2017.87

72. Sprocati AR, Alisi C, Tasso F, et al (2014) Bioprospecting at former mining sites across Europe: microbial and functional diversity in soils. Environ Sci Pollut Res Int 21:6824–6835. doi: 10.1007/s11356-013-1907-3

73. Ellis RJ, Morgan P, Weightman AJ, Fry JC (2003) Cultivation-Dependent and -Independent Approaches for Determining Bacterial Diversity in Heavy-Metal-Contaminated Soil. Appl Environ Microbiol 69:3223–3230. doi: 10.1128/AEM.69.6.3223-3230.2003

74. Giller KE, Witter E, Mcgrath SP (1998) Toxicity of heavy metals to microorganisms and microbial processes in agricultural soils: a review. Soil Biol Biochem 30:1389–1414. doi: 10.1016/S0038-0717(97)00270-8

75. Hemme CL, Deng Y, Gentry TJ, et al (2010) Metagenomic insights into evolution of a heavy metal-contaminated groundwater microbial community. ISME J 4:660–672. doi: 10.1038/ismej.2009.154

76. Chander K, Joergensen RG (2001) Decomposition of 14C glucose in two soils with different amounts of heavy metal contamination. Soil Biol Biochem 33:1811–1816. doi: 10.1016/S0038-0717(01)00108-0

77. Preston-Mafham J, Boddy L, Randerson PF (2002) Analysis of microbial community functional diversity using sole-carbon-source utilisation profiles – a critique. FEMS Microbiol Ecol 42:1–14 . doi: 10.1016/S0168-6496(02)00324-0

78. Lock K, Janssen CR (2005) Influence of soil zinc concentrations on zinc sensitivity and functional diversity of microbial communities. Environ Pollut Barking Essex 1987 136:275–281. doi: 10.1016/j.envpol.2004.12.038

79. Ni N, Wang F, Song Y, et al (2017) Effects of cationic surfactant on the bioaccumulation of polycyclic aromatic hydrocarbons in rice and the soil microbial community structure. RSC Adv 7:41444–41451. doi: 10.1039/C7RA07124H

80. Ren G, Teng Y, Ren W, et al (2016) Pyrene dissipation potential varies with soil type and associated bacterial community changes. Soil Biol Biochem 103:71–85. doi: 10.1016/j.soilbio.2016.08.007

81. Padmanabhan P, Padmanabhan S, DeRito C, et al (2003) Respiration of 13C-Labeled Substrates Added to Soil in the Field and Subsequent 16S rRNA Gene Analysis of 13C-Labeled Soil DNA. Appl Environ Microbiol 69:1614–1622. doi: 10.1128/AEM.69.3.1614-1622.2003

82. Trzesicka-Mlynarz D, Ward OP (1995) Degradation of polycyclic aromatic hydrocarbons (PAHs) by a mixed culture and its component pure cultures, obtained from PAH-contaminated soil. Can J Microbiol 41:470–476.

83. Viñas M, Sabaté J, Espuny MJ, Solanas AM (2005) Bacterial Community Dynamics and Polycyclic Aromatic Hydrocarbon Degradation during Bioremediation of Heavily Creosote-

953 Contaminated Soil. Appl Environ Microbiol 71:7008–7018. doi: 10.1128/AEM.71.11.7008-
954 7018.2005

955 84. Martirani-Von Abercron S, Marín P, Solsona-Ferraz M, et al (2017) Naphthalene
956 biodegradation under oxygen-limiting conditions: community dynamics and the relevance of
957 biofilm-forming capacity. Microb Biotechnol 10:1781–1796. doi: 10.1111/1751-7915.12842

958 85. Cébron A, Beguiristain T, Faure P, et al (2009) Influence of Vegetation on the In Situ Bacterial
959 Community and Polycyclic Aromatic Hydrocarbon (PAH) Degraders in Aged PAH-Contaminated
960 or Thermal-Desorption-Treated Soil. Appl Environ Microbiol 75:6322–6330. doi:
961 10.1128/AEM.02862-08

962 86. Rousk J, Bååth E, Brookes PC, et al (2010) Soil bacterial and fungal communities across a pH
963 gradient in an arable soil. ISME J 4:1340–1351. doi: 10.1038/ismej.2010.58

964 87. Brewer TE, Handley KM, Carini P, et al (2017) Genome reduction in an abundant and
965 ubiquitous soil bacterium '*Candidatus* Udaeobacter copiosus.' Nat Microbiol 2:16198. doi:
966 10.1038/nmicrobiol.2016.198

967 88. Sessitsch A, Weilharter A, Gerzabek MH, et al (2001) Microbial population structures in soil
968 particle size fractions of a long-term fertilizer field experiment. Appl Environ Microbiol
969 67:4215–4224. doi: 10.1128/AEM.67.9.4215-4224.2001

970 89. Franzluebbers AJ, Haney RL, Hons FM, Zuberer DA (1996) Active fractions of organic matter in
971 soils with different texture. Soil Biol Biochem 28:1367–1372. doi: 10.1016/S0038-
972 0717(96)00143-5

973 90. Chau JF, Bagtzoglou AC, Willig MR (2011) The Effect of Soil Texture on Richness and Diversity
974 of Bacterial Communities. Environ Forensics 12:333–341 . doi:
975 10.1080/15275922.2011.622348

976 91. Kandeler F, Kampichler C, Horak O (1996) Influence of heavy metals on the functional diversity
977 of soil microbial communities. Biol Fertil Soils 23:299–306. doi: 10.1007/BF00335958

978 92. Valsecchi G, Gigliotti C, Farini A (1995) Microbial biomass, activity, and organic matter
979 accumulation in soils contaminated with heavy metals. Biol Fertil Soils 20:253–259. doi:
980 10.1007/BF00336086

981 93. Chew I, Obbard JP, Stanforth RR (2001) Microbial cellulose decomposition in soils from a rifle
982 range contaminated with heavy metals. Environ Pollut 111:367–375. doi: 10.1016/S0269-
983 7491(00)00094-4

984 94. McEnroe NA, Helmisaari H-S (2001) Decomposition of coniferous forest litter along a heavy
985 metal pollution gradient, south-west Finland. Environ Pollut 113:11–18. doi: 10.1016/S0269-
986 7491(00)00163-9

987 95. Lucisine P, Lecerf A, Danger M, et al (2015) Litter chemistry prevails over litter consumers in
988 mediating effects of past steel industry activities on leaf litter decomposition. Sci Total Environ
989 537:213–224. doi: 10.1016/j.scitotenv.2015.07.112

990 96. Wardle DA (1992) A Comparative Assessment of Factors Which Influence Microbial Biomass
991 Carbon and Nitrogen Levels in Soil. Biol Rev 67:321–358. doi: 10.1111/j.1469-
992 185X.1992.tb00728.x

993 97. Johnson D, Leake JR, Lee JA, Campbell CD (1998) Changes in soil microbial biomass and
994 microbial activities in response to 7 years simulated pollutant nitrogen deposition on a
995 heathland and two grasslands. Environ Pollut 103:239–250. doi: 10.1016/S0269-
996 7491(98)00115-8

997 98. Kuperman RG, Carreiro MM (1997) Soil heavy metal concentrations, microbial biomass and
998 enzyme activities in a contaminated grassland ecosystem. Soil Biol Biochem 29:179–190. doi:
999 10.1016/S0038-0717(96)00297-0

1000 99. Moore A, Becking J (1963) Nitrogen Fixation by Bacillus Strains Isolated from Nigerian Soils.
1001 Nature 198:915-916. doi: 10.1038/198915a0

1002 100. Fierer N, Lauber CL, Ramirez KS, et al (2012) Comparative metagenomic, phylogenetic and
1003 physiological analyses of soil microbial communities across nitrogen gradients. ISME J 6:1007–
1004 1017. doi: 10.1038/ismej.2011.159

1005

1006

1007 **Table 1.**

			Mo	He	Di	Uc	Te	NM	Ho	Po	MsM	RM	Means (± SE) per group Kruskall-Wallis multiple comparaison test (95% confidence)		
Soil group			ctrl	ctrl	ctrl	sh	sh	sh	sh	sp	sp	sp	ctrl	sh	sp
Total organic carbon (g kg^{-1})			81.5	72.1	24.3	29.9	88.2	75.2	159.0	109.0	119.0	149.0	59.3 ± 17.7	88.1 ± 26.7	125.7 ± 12.0
Dissolved organic carbon (g kg^{-1})			1.34	1.69	1.18	0.12	0.99	0.23	0.33	0.76	0.66	0.24	1.4 ± 0.2 [a]	0.4 ± 0.2 [b]	0.6 ± 0.2 [b]
Organic matter (g kg^{-1})			141	125	42	52	153	130	276	189	206	257	102.7 ± 30.7	152.7 ± 46.5	217.3 ± 20.4
Nitrogen (g kg^{-1})			4.56	2.85	1.74	0.56	4.35	2.35	2.92	7.19	4.18	3.83	3.1 ± 0.8	2.5 ± 0.8	5.1 ± 1.1
C/N			17.9	25.3	14.0	53.6	20.3	32.0	54.6	15.2	28.5	38.8	19.1 ± 3.3	40.1 ± 8.4	27.5 ± 6.8
Available phosphorus (g kg^{-1})			0.04	0.02	0.04	< 0.01	0.21	0.08	0.02	0.12	0.21	0.07	0.03 ± 0.01	0.08 ± 0.05	0.13 ± 0.04
CEC (cmol kg^{-1})			35.0	15.5	9.9	3.6	20.0	17.5	9.8	51.2	16.2	10.8	20.1 ± 7.6	12.7 ± 3.7	26.1 ± 12.7
Carbonates (g kg^{-1})			5.5	0.8	14.3	8.4	181.8	14.2	114.0	89.6	152.0	219.3	6.9 ± 3.9	79.6 ± 41.8	153.7 ± 37.4
pH (H_2O)			7.0	5.4	7.3	8.0	7.7	7.4	7.5	7.8	7.2	7.6	6.6 ± 0.6	7.6 ± 0.1	7.6 ± 0.2
Organic acids (mg kg^{-1})			222.9	140.0	120.7	43.2	179.0	11.5	238.1	279.3	154.0	114.2	161.2 ± 31.4	118.0 ± 54.1	182.5 ± 49.7
Carbohydrates (mg kg^{-1})			0.28	0.29	0.10	0.04	0.20	0.02	0.05	0.08	0.05	0.07	0.22 ± 0.06	0.08 ± 0.04	0.07 ± 0.01
Soil texture (%)		Clay	48.9	25.5	11.5	5.5	10.0	13.3	7.0	17.5	10.9	10.9	28.6 ± 10.9	9.0 ± 1.7	13.1 ± 2.2
		Silt	46.0	69.0	14.3	17.6	20.7	27.9	12.0	53.3	72.7	74.6	43.1 ± 15.9	19.6 ± 3.3	66.9 ± 6.8
		Sand	5.1	5.5	74.2	76.9	69.3	58.8	81.0	29.2	16.4	14.5	28.3 ± 23.0	71.5 ± 4.9	20.0 ± 4.6
Total concentration (hydrofluoric acid extraction)	Major elements (g kg^{-1})	Al	67.2	51.9	45.0	19.9	25.5	39.9	40.0	39.6	21.0	22.0	5.5 ± 0.7 [a]	3.1 ± 0.5 [b]	2.8 ± 0.6 [b]
		Ca	16.2	3.8	11.6	46.7	125.0	99.2	151.0	71.9	88.1	129.0	1.1 ± 0.4	10.5 ± 2.2	9.6 ± 1.7
		K	14.6	18.6	28.6	0.6	5.4	9.2	5.8	5.4	1.5	3.4	2.1 ± 0.4 [a]	0.5 ± 0.2 [b]	0.3 ± 0.1 [b]
		Mg	5.8	4.8	3.2	5.9	23.5	7.4	9.9	11.3	4.3	3.9	0.5 ± 0.1	1.2 ± 0.4	0.6 ± 0.2
		Na	2.52	5.87	8.87	0.40	1.61	2.73	1.49	0.76	0.40	0.28	0.58 ± 0.18	0.16 ± 0.05	0.05 ± 0.01
		Fe *	44.1	27.3	18.0	452.0	108.0	193.0	65.8	93.0	304.0	53.6	3.0 ± 0.8 [b]	20.5 ± 8.7 [a]	15.0 ± 7.8 [a]
	Metallic trace elements (mg kg^{-1})	Zn *	144	248	60.5	74	1 650	2 540	314	29 600	55 400	119 000	151 ± 54 [b]	1 144 ± 580 [b]	68 000 ± 26 565 [a]
		Pb *	44	93	31	23	475	653	303	34 700	14 400	39 500	56 ± 19 [b]	363 ± 134 [b]	29 533 ± 7 692 [a]
		Cd *	0.7	0.3	0.1	0.1	4.5	3.3	1.1	152.0	17.6	22.0	0.4 ± 0.2 [b]	2.2 ± 1.0 [b]	63.9 ± 44.1 [a]
		Cr *	75.1	82.1	18.7	22.5	345.0	1 220.0	177.0	150.0	166.0	61.9	58.6 ± 20.1	441.1 ± 267.8	126.0 ± 32.4
		Cu *	16.4	12.9	10.2	9.4	146.0	144.0	93.6	148.0	186.0	42.3	13.2 ± 1.8	98.3 ± 32.0	125.4 ± 43.0
		Ni *	42.5	21.7	13.2	7.3	55.3	113.0	29.9	73.1	246.0	34.3	25.8 ± 8.7	51.4 ± 22.8	117.8 ± 65.1
		Co *	14.2	19.0	4.8	17.4	20.2	28.8	11.3	10.6	51.4	11.3	12.7 ± 4.2	19.4 ± 3.6	24.4 ± 13.5
		Tl *	0.77	0.59	1.13	0.09	0.52	0.83	0.26	88.30	4.79	8.63	0.83 ± 0.16 [b]	0.43 ± 0.16 [b]	33.91 ± 27.22 [a]
		Mo	1.5	0.9	0.5	0.6	4.6	12.3	10.0	7.9	21.0	1.5	1.0 ± 0.3	6.9 ± 2.6	10.1 ± 5.7
		Mn	932	1 570	285	740	3 480	9 890	2 520	68 100	3 830	771	929 ± 371	4 158 ± 1 993	24 234 ± 21 951
Available concentration (calcium chloride extraction; µg kg^{-1})		Zn	< 10	38 100	11	< 10	36	128	38	2 310	49 200	64 000	12 704 ± 12 698	51 ± 27	38 503 ± 18 594
		Pb	< 3	94	< 3	< 3	< 3	< 3	< 3	32	397	1 440	32 ± 31 [b]	1 ± 0 [b]	623 ± 422 [a]
		Cd	2.3	82.8	1.3	< 1.0	1.6	2.4	1.7	48.7	111.0	25.3	28.8 ± 27.0	1.7 ± 0.3	61.7 ± 25.6
		Cr	< 10	< 10	< 10	< 10	< 10	20	< 10	29	< 10	< 10	1 ± 0	5.7 ± 4.7	10.5 ± 9.5
		Cu	41	30	27	24	129	84	237	98	187	29	33 ± 4	118 ± 45	105 ± 46
		Ni	< 15	390	< 15	< 15	< 15	90	< 15	< 15	126	59	131 ± 130	23 ± 22	62 ± 36
Metal pollution index			71.2	66.8	27.2	144.0	198.6	329.0	115.6	475.5	480.9	299.8	55.1 ± 14.0 [c]	196.8 ± 47.3 [b]	418.7 ± 59.5 [a]
Sum of 16 regulatory PAH (n = 3; mg kg^{-1})		Total	3.5	0.1	0.9	0.9	114.7	1 095.9	937.7	21.2	49.6	6.6	1.5 ± 0.6 [b]	537.3 ± 146.2 [a]	25.8 ± 6.4 [a]
		Available	0.0	0.0	0.0	0.0	6.3	83.0	54.1	0.2	4.6	0.0	0.0 ± 0.0 [c]	35.8 ± 10.7 [a]	1.6 ± 0.8 [b]

1008
1009
1010

Table 2.

		Mo	He	Di	Uc	Te	NM	Ho	Po	MsM	RM	Means (± SE) per group Kruskall-Wallis multiple comparaison test (95% confidence)		
	Soil group	ctrl	ctrl	ctrl	sh	sh	sh	sh	sp	sp	sp	ctrl	sh	sp
Microbial characteristics (n = 3)	MPN ($x10^3$ g^{-1})	1 434.5 ± 327.7	40.2 ± 8.1	488.6 ± 126.1	161.2 ± 53.9	586.1 ± 170.0	496.9 ± 214.8	2 071.4 ± 952.1	80.2 ± 19.1	38.5 ± 4.1	0.1 ± 0.1	654.5 ± 410.9	828.9 ± 424.1	39.6 ± 23.1
	16S rRNA gene copy number ($x10^{10}$ g^{-1})	17.8 ± 2.4	25.0 ± 2.2	30.1 ± 1.1	6.9 ± 0.5	41.5 ± 1.2	4.4 ± 0.3	14.8 ± 0.7	41.5 ± 0.4	26.4 ± 1.2	17.8 ± 0.4	24.3 ± 2.1	16.9 ± 4.5	28.6 ± 3.5
	18S/16S rRNA gene copy ratio	0.03 ± 0.00	0.18 ± 0.01	0.07 ± 0.00	0.08 ± 0.01	0.08 ± 0.01	0.07 ± 0.01	0.08 ± 0.00	0.04 ± 0.00	0.04 ± 0.00	0.05 ± 0.00	0.09 [a] ± 0.02	0.08 [a] ± 0.00	0.04 [b] ± 0.00
Bacterial taxonomic diversity (n = 3)	Chao1 index	2 621 ± 205	3,161 ± 254	4 966 ± 32	4 293 ± 291	4 380 ± 38	2 541 ± 100	4 966 ± 100	3 422 ± 223	3 151 ± 2	2 478 ± 15	3,583 ± 367	4 045 ± 282	3 017 ± 154
	Shannon's index (H')	5.40 ± 0.03	6.38 ± 0.05	7.12 ± 0.02	6.68 ± 0.03	6.97 ± 0.01	6.37 ± 0.01	7.06 ± 0.04	6.65 ± 0.02	6.06 ± 0.02	5.99 ± 0.02	6.30 [ab] ± 0.25	6.77 [a] ± 0.08	6.23 [b] ± 0.11
	Pielou's evenness index (J')	0.70 ± 0.01	0.80 ± 0.01	0.85 ± 0.01	0.81 ± 0.00	0.84 ± 0.00	0.82 ± 0.00	0.84 ± 0.00	0.83 ± 0.00	0.77 ± 0.00	0.78 ± 0.00	0.78 [ab] ± 0.02	0.83 [a] ± 0.00	0.79 [b] ± 0.01
MicroResp catabolic diversity (n = 4)	Catabolic richness (n = 6)	5.0 ± 0.0	5.8 ± 0.3	5.0 ± 0.0	5.8 ± 0.3	4.5 ± 0.3	5.0 ± 0.4	4.5 ± 0.3	5.8 ± 0.3	5.0 ± 0.4	4.5 ± 0.3	5.3 ± 0.2	4.9 ± 0.2	5.1 ± 0.3
	Shannon's index (H')	1.53 ± 0.03	1.62 ± 0.06	1.57 ± 0.01	1.72 ± 0.05	1.41 ± 0.07	1.57 ± 0.08	1.49 ± 0.07	1.13 ± 0.02	1.41 ± 0.09	1.39 ± 0.07	1.57 [a] ± 0.03	1.55 [a] ± 0.05	1.31 [b] ± 0.06
	Pielou's evenness index (J')	0.95 ± 0.02	0.93 ± 0.02	0.97 ± 0.01	0.98 ± 0.00	0.94 ± 0.02	0.98 ± 0.01	0.99 ± 0.00	0.65 ± 0.02	0.88 ± 0.03	0.93 ± 0.01	0.95 [b] ± 0.01	0.97 [a] ± 0.01	0.82 [c] ± 0.04
Biolog catabolic diversity (n = 3)	Catabolic richness (n = 62)	30.7 ± 1.3	17.7 ± 2.2	21.3 ± 1.45	25.7 ± 2.6	22.0 ± 9.5	12.7 ± 3.5	15.7 ± 5.8	15.0 ± 1.5	12.0 ± 4.4	5.0 ± 1.15	23.2 [a] ± 2.1	19.0 [a] ± 3.0	10.7 [b] ± 2.0
	Shannon index (H')	3.27 ± 0.04	2.77 ± 0.13	2.97 ± 0.07	3.15 ± 0.10	2.78 ± 0.38	2.35 ± 0.36	2.43 ± 0.41	2.47 ± 0.09	2.22 ± 0.39	1.52 ± 0.25	3.00 [a] ± 0.08	2.68 [a] ± 0.17	2.07 [b] ± 0.20
	Pielou's evenness index (J')	0.96 ± 0.00	0.97 ± 0.01	0.97 ± 0.00	0.97 ± 0.01	0.95 ± 0.01	0.96 ± 0.02	0.94 ± 0.01	0.92 ± 0.02	0.95 ± 0.01	0.98 ± 0.01	0.97 ± 0.00	0.95 ± 0.01	0.95 ± 0.01

1014 Figure 1.

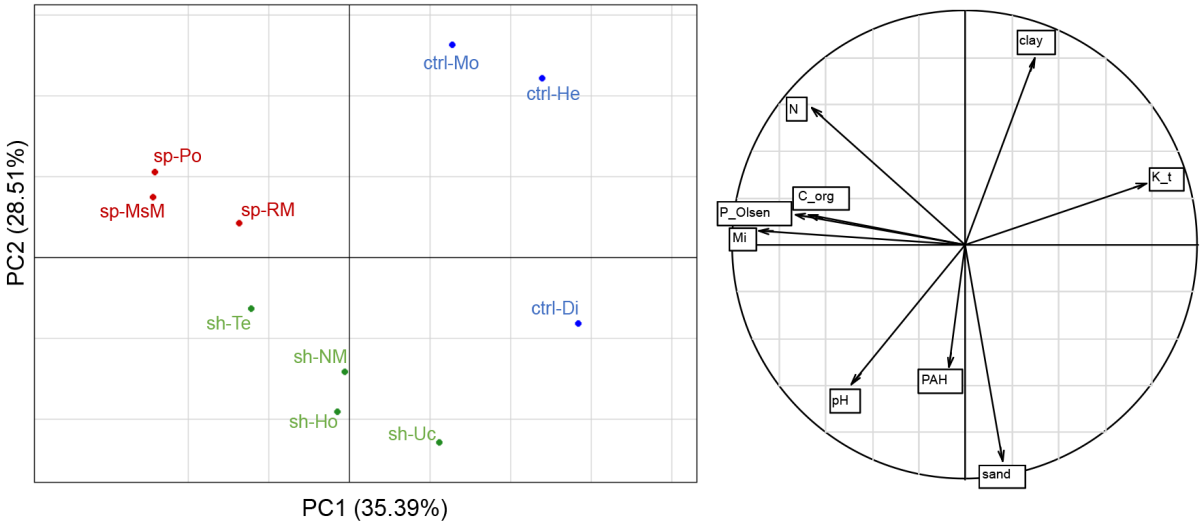

1015

1016

Figure 2.

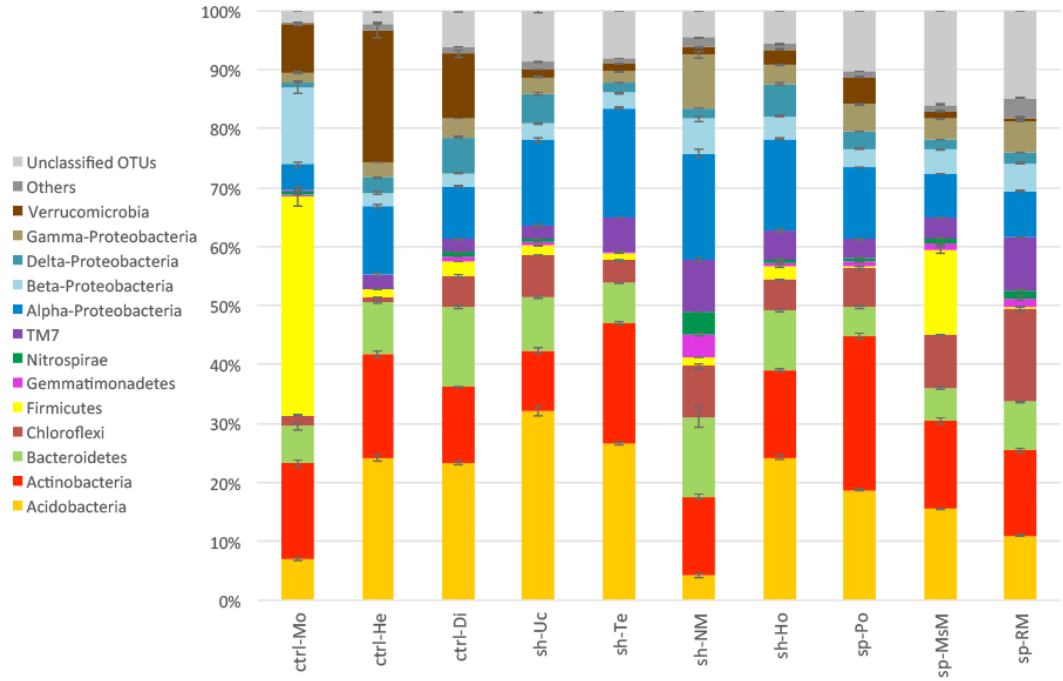

	Control	Slag heap	Settling pond	p-value
Unclassified OTUs	C	B	A	2.100×10^{-5}
Others		n.s.		0.661
Verrucomicrobia	A	B	B	9.415×10^{-5}
Gamma-proteobacteria	C	B	A	2.793×10^{-3}
Delta-proteobacteria		n.s.		0.404
Beta-proteobacteria		n.s.		0.325
Alpha-proteobacteria	B	A	B	2.840×10^{-5}
Candidate div. TM7	B	A	A	1.103×10^{-3}
Nitrospirae	B	B	A	9.559×10^{-3}
Gemmatimonadetes	C	B	A	5.512×10^{-5}
Firmicutes		n.s.		0.084
Chloroflexi	C	B	A	1.989×10^{-4}
Bacteroidetes	A	A	B	2.967×10^{-3}
Actinobacteria		n.s.		0.396
Acidobacteria		n.s.		0.086

Figure 3.

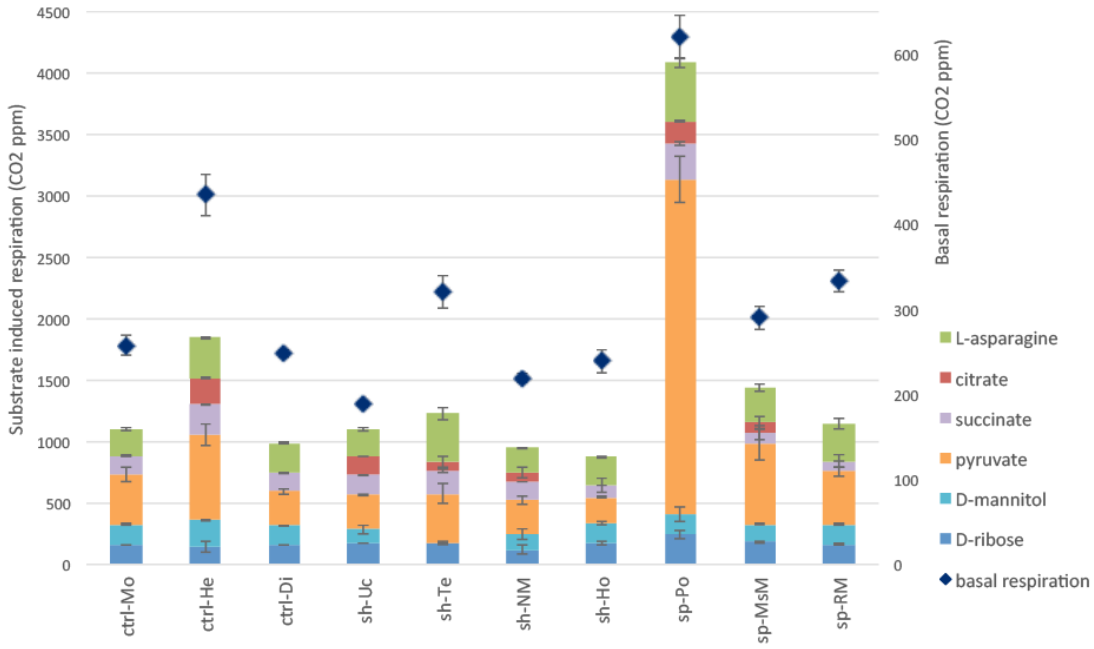

	Control	Slag heap	Settling pond	p-Value
Sum of SIRs	B	B	A	1.983×10^{-3}
L-asparagine	AB	B	A	0.037
Citrate		n.s.		0.754
Succinate		n.s.		0.753
Pyruvate	B	C	A	9.542×10^{-5}
D-mannitol	A	AB	C	0.021
D-ribose		n.s.		0.163
Basal respiration	B	C	A	1.733×10^{-7}

Figure 4.

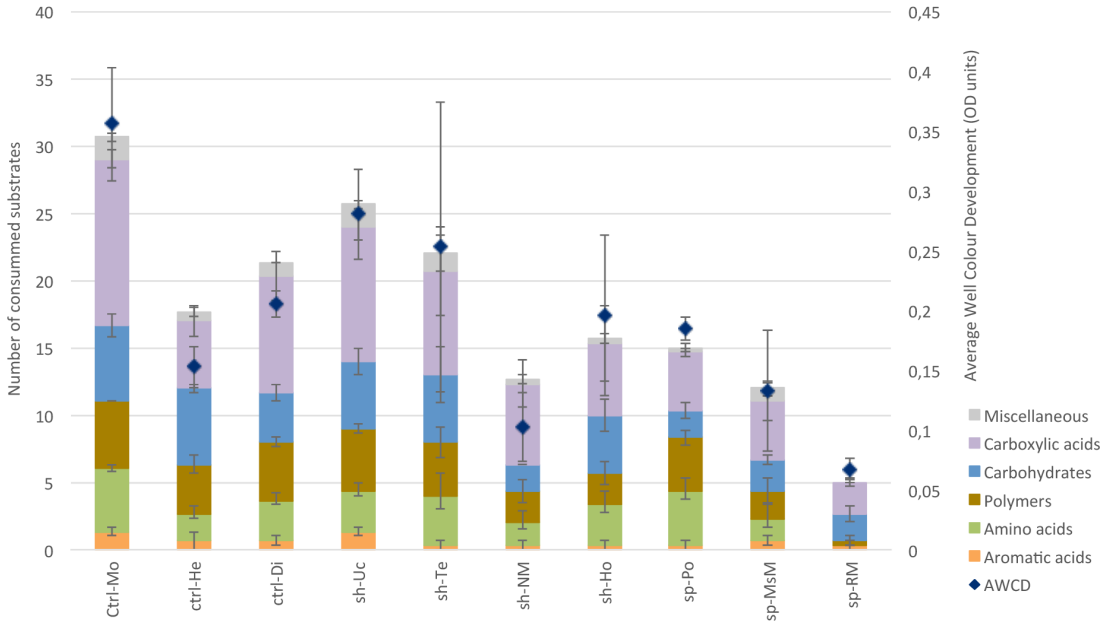

	Control	Slag heap	Settling pond	p-Value
Total richness	A	A	B	0.007
Miscellaneous		n.s.		0.146
Carboxylic acids	A	A	B	0.017
Carbohydrates	A	A	B	0.004
Polymers	A	AB	B	0.032
Amino acids		n.s.		0.289
Aromatic acids		n.s.		0.421
AWCD 96h		n.s.		0.078

1026 **Figure 5.**

1027

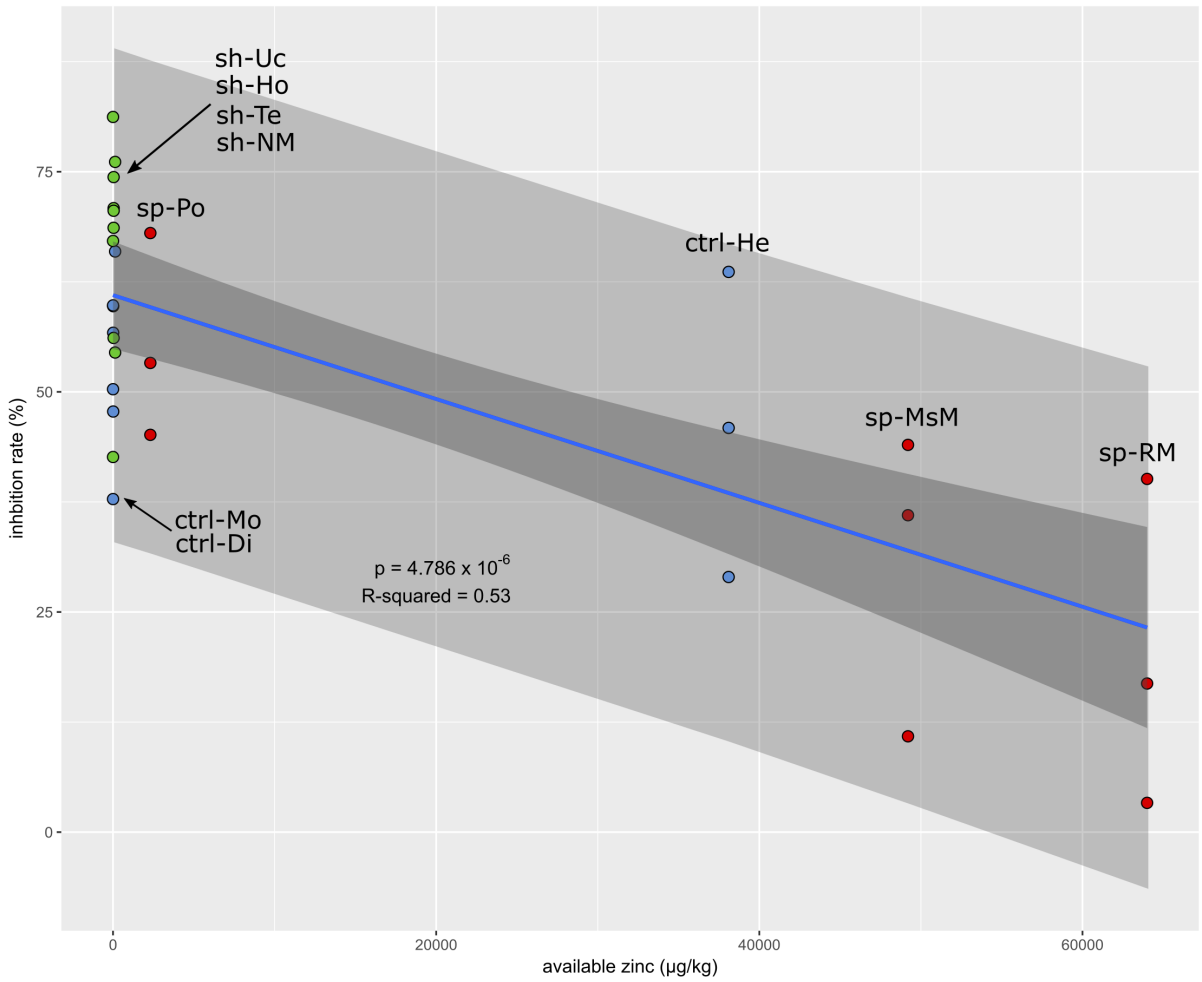

1028

1029

Figure 6.

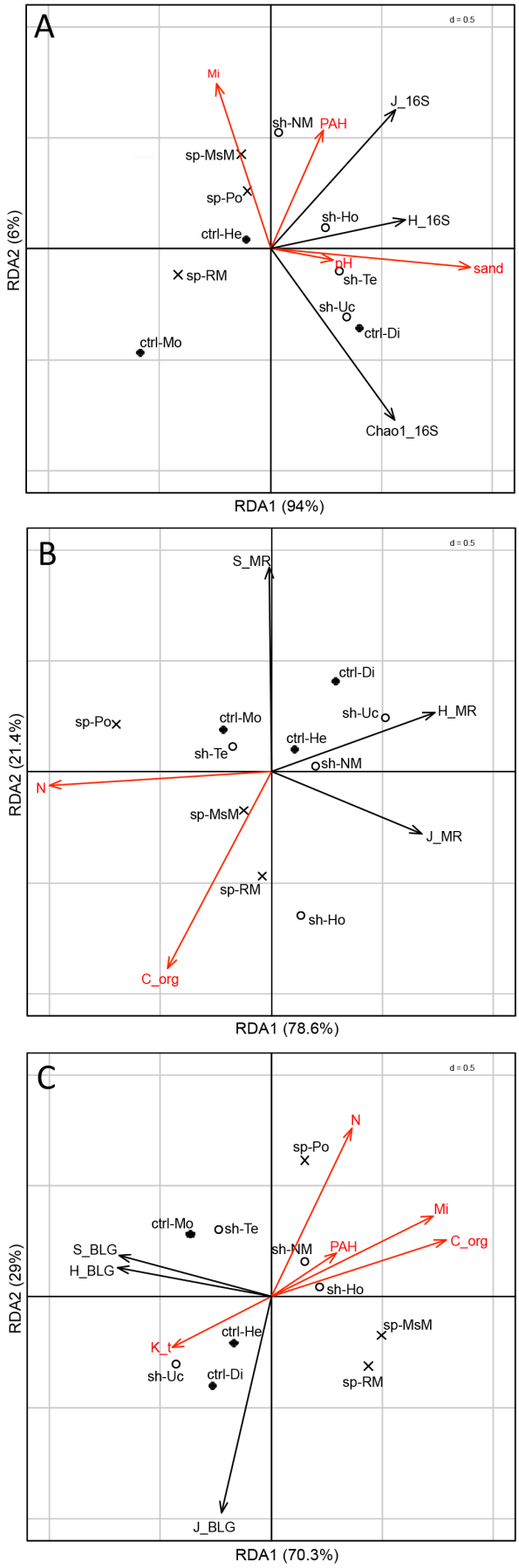
A
d = 0.5
Mi
J_16S
sh-NM
PAH
sp-MsM
sp-Po
sh-Ho
H_16S
ctrl-He
pH
sand
sp-RM
sh-Te
sh-Uc
ctrl-Di
ctrl-Mo
Chao1_16S
RDA2 (6%)
RDA1 (94%)
B
d = 0.5
S_MR
ctrl-Di
sp-Po
ctrl-Mo
sh-Uc
H_MR
ctrl-He
sh-Te
sh-NM
N
sp-MsM
J_MR
sp-RM
sh-Ho
C_org
RDA2 (21.4%)
RDA1 (78.6%)
C
d = 0.5
N
sp-Po
ctrl-Mo
sh-Te
Mi
C_org
S_BLG
H_BLG
sh-NM
PAH
sh-Ho
sp-MsM
ctrl-He
K_t
sh-Uc
ctrl-Di
sp-RM
J_BLG
RDA2 (29%)
RDA1 (70.3%)

1032

Supplementary material

Figure S1.

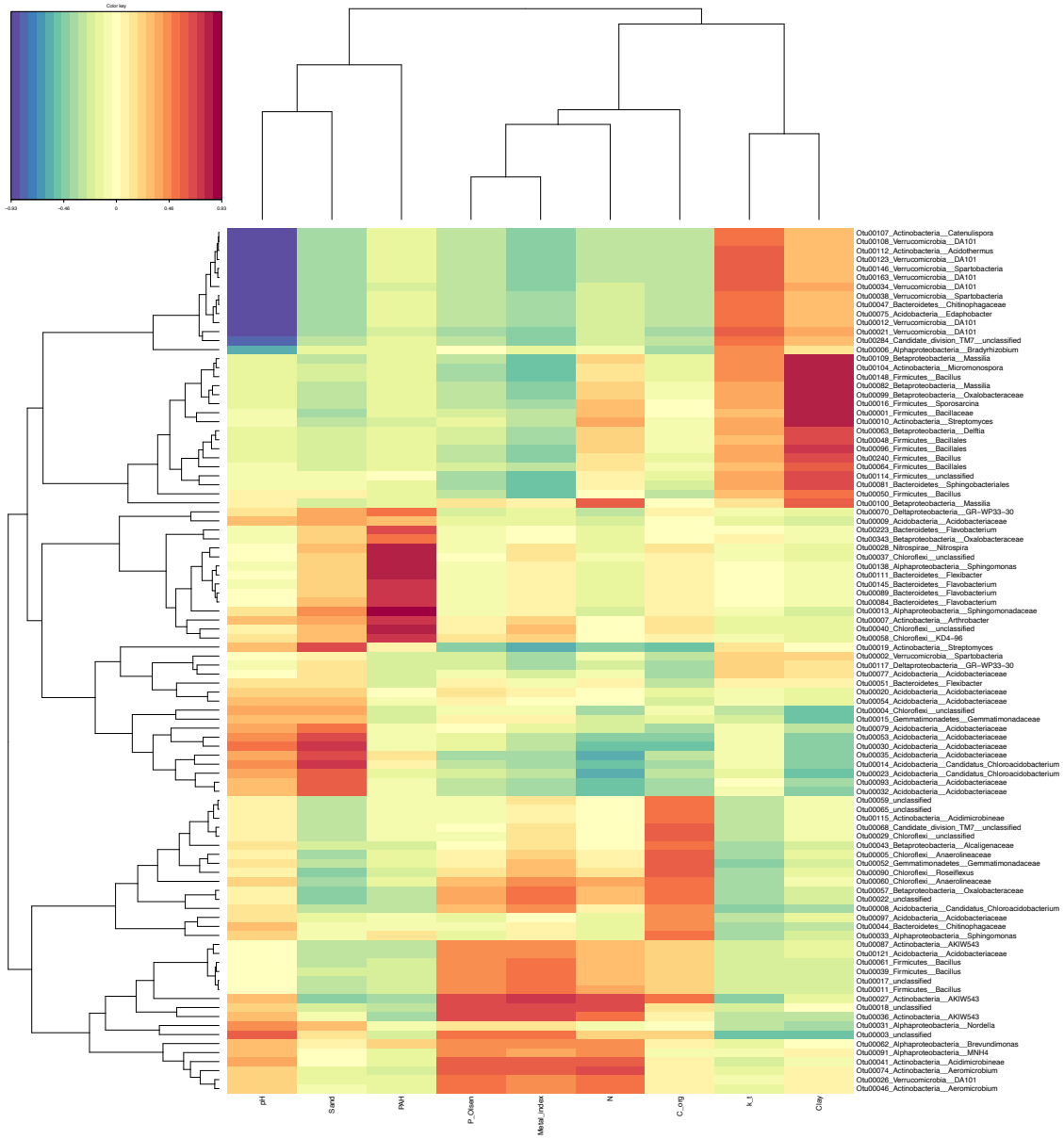

Table S1.

			Biolog		MicroResp	
Chemical guild	**Substrate**	**Chemical formula**	**Eco**	**MT2**	**Substrate**	**Time (h)**
PAHs	Phenanthrene	$C_{14}H_{10}$		✓		
	Pyrene	$C_{16}H_{10}$		✓		
	Fluoranthene	$C_{16}H_{10}$		✓		
	Fluorene	$C_{13}H_{10}$		✓		
Aromatic acids	Benzoïc acid	$C_7H_6O_2$		✓		
	Protocatechuic acid	$C_7H_6O_4$		✓		
	Phtalic acid	$C_8H_6O_4$		✓		
	P-Coumaric acid	$C_9H_8O_3$		✓		
	Ferulic acid	$C_{10}H_{10}O_4$		✓		
	Syringic acid	$C_9H_{10}O_5$		✓		
Carboxylic acids	Pyruvic acid	$C_3H_4O_3$		✓	✓	4.67
	Propionic acid	$C_3H_6O_2$		✓		
	D-Gluconic acid	$C_6H_{12}O_7$		✓		
	Oxalic acid	$C_2H_2O_4$		✓		
	Succinic acid	$C_4H_6O_4$		✓	✓	6.67
	Citric acid	$C_6H_8O_7$		✓	✓	6.17
	Trans-Aconitic acid	$C_6H_6O_6$		✓		
	L-Tartaric acid	$C_4H_6O_6$		✓		
	D-Galactonic acid γ-lactone	$C_6H_{10}O_6$	✓			
	D-Galacturonic acid	$C_6H_{10}O_7$	✓			
	γ-Hydroxybutyric acid	$C_4H_8O_3$	✓			
	D-Glucosaminic acid	$C_6H_{13}NO_6$	✓			
	Itaconic acid	$C_5H_6O_4$	✓			
	α-Ketobutyric acid	$C_4H_6O_3$	✓			
	D-Malic acid	$C_4H_6O_5$	✓			
	2-Hydroxy benzoic acid	$C_7H_6O_3$	✓			
	4-Hydroxy benzoic acid	$C_7H_6O_3$	✓			
Amino acids	L-Proline	$C_5H_9NO_2$		✓		
	Glycine	$C_2H_5NO_2$		✓		
	L-Alanine	$C_3H_7NO_2$		✓		
	L-Arginine	$C_6H_{14}N_4O_2$	✓			
	L-Asparagine	$C_4H_8N_2O_3$	✓		✓	5.33
	L-Phenylalanine	$C_9H_{11}NO_2$	✓			
	L-Serine	$C_3H_7NO_3$	✓			
	L-Threonine	$C_4H_9NO_3$	✓			
	Glycyl-L-Glutamic Acid	$C_7H_{12}N_2O_5$	✓			
Carbohydrates	D-Ribose	$C_5H_{10}O_5$		✓	✓	8.00
	D-Glucose	$C_6H_{12}O_6$		✓		
	D-Fructose	$C_6H_{12}O_6$		✓		
	D-Sucrose	$C_{12}H_{22}O_{11}$		✓		
	D-Trehalose	$C_{12}H_{22}O_{11}$		✓		
	D-Mannose	$C_6H_{12}O_6$		✓		
	β-Methyl-D-glucoside	$C_7H_{14}O_6$	✓			
	D-Xylose	$C_5H_{10}O_5$	✓			
	i-Erythritol	$C_4H_{10}O_4$	✓			
	D-Mannitol	$C_6H_{14}O_6$	✓		✓	8.17
	N-Acetyl-D-glucosamine	$C_8H_{15}NO_6$	✓			
	D-Cellobiose	$C_{12}H_{22}O_{11}$	✓			
	α-D-Lactose	$C_{12}H_{22}O_{11}$	✓			
	Pyruvic acid methyl ester	$C_4H_6O_3$	✓			
Polymers	Lignin (alkali)	$(C_{14}H_{20}O_3S)_n$		✓		
	Cellulose (from Spruce)	$(C_6H_{10}O_5)_n$		✓		
	Xylan	$(C5H8O5)_n$		✓		
	Glycogen	$(C_6H_{10}O_5)_n$	✓			
	α-Cyclodextrine	$C_{36}H_{60}O_{30}$	✓			
	Tween 40		✓			
	Tween 80		✓			
Miscellaneous	Glucose-1-phosphate	$C_6H_{13}O_9P$	✓			
	D,L-α-Glycerol phosphate	$C_3H_9O_6P$	✓			
	Phenylethyl-amine	$C_8H_{11}N$	✓			
	Putrescine	$C_4H_{12}N_2$	✓			
	Catechol	$C_6H_6O_2$		✓		

classement d'après Analysis of microbial community functional diversity using sole-carbon-source utilisation profiles - a critique (Preston-Mafham et al. 2002) avec changement de groupes (*) ou ajout (#)

1043 Table S2.

		F-value	P-value	
RDA-A	Axis 1	26.338	0.001	***
	Axis 2	1.683	0.216	
	Ti_metals	2.072	0.198	
	PAH	1.729	0.238	
	sand	16.304	0.002	**
	pH	3.251	0.108	
RDA-B	Axis 1	10.353	0.002	**
	Axis 2	2.815	0.111	
	C_org	4.458	0.009	**
	N	8.709	0.002	**
RDA-C	Axis 1	19.903	0.002	**
	Axis 2	8.222	0.012	*
	Ti_metals	7.767	0.010	**
	PAH	1.047	0.412	
	C_org	2.963	0.110	
	N	4.708	0.032	*
	K_t	2.396	0.139	

$p < 0.05$	*
$p < 0.01$	**
$p < 0.001$	***

1044

1045